nature portfolio

Peer Review File

Spin-conserved oxygen-redox coupling enables durable anion exchange membrane water electrolysis

Corresponding Author: Professor Junmin Xue

This file contains all reviewer reports in order by version, followed by all author rebuttals in order by version.

Version 0:

Reviewer comments:

Reviewer #1

(Remarks to the Author)
This study focuses on the design of cascade-reconstructed CoOOH derived from SC-ROC for high-performance anion exchange membrane water electrolysis. The research idea is clear, the characterization is relatively comprehensive, and the catalytic performance is satisfactory. However, there still exist considerable uncertainties in the experimental setup and mechanism interpretation, which require careful revision and improvement by the authors.
1. In this system, Pt foil is used as the counter electrode in all the three-electrode systems adopted by the author. The oxidation of V-CoS_2 takes as long as 10 hours. Under such prolonged exposure to a strong alkaline environment, trace amounts of Pt may be etched and subsequently deposited and adsorbed onto the surface of the working electrode, thereby leading to an enhancement in catalytic performance. The author is advised to repeat the experiment using a carbon rod or carbon plate as the counter electrode to verify whether the same performance can be achieved.
2. In this system, the authors confirm that the catalyst simultaneously generates oxygen vacancies and metal defects. Which of these two types of defects plays a dominant role? Could the authors provide experimental evidence to clarify this? Meanwhile, how significantly do different oxidative etching durations affect the catalytic performance? In addition, why did the authors specifically select an etching time of 10 hours?
3. The conclusion emphasizes that SC-ROC is a universal design principle, but it has only been validated in a Co-based system. Please briefly discuss the applicability of this strategy to other transition metal systems (e.g., Ni, Fe) to strengthen the scientific significance.
4. Please supplement a comprehensive comparison of the OER performance (overpotential and Tafel slope) of this catalyst with state-of-the-art OER catalysts reported in recent literature.
5. For the as-prepared CR-CoOOH catalyst, the influence of the vanadium component cannot be ruled out, and the contribution of trace vanadium to the catalytic performance needs to be evaluated. Moreover, the theoretical calculation model established by the authors also fails to take the effect of V into account.
6. The precursors of CR-CoOOH and LR-CoOOH (i.e., V-CoS_2 and CoS_2) exhibit obvious differences in microstructure and XPS peak profiles. It is necessary to clarify whether such differences serve as a key factor leading to the performance discrepancy of the derived catalysts.

Reviewer #2

(Remarks to the Author)
Li and coauthors reported a cascade-reconstructed CoOOH (CR-CoOOH) catalyst that enables a spin-conserved radical oxygen coupling (SC-ROC) pathway for the oxygen evolution reaction (OER). By combining operando spectroscopy, magnetic characterization, isotope-labeled DEMS, and electrochemical measurements, the authors provide a relatively comprehensive dataset supporting the involvement of oxygen-redox chemistry. In addition, the work demonstrates impressive device-level performance. Overall, the manuscript is of considerable interest. However, several important issues remain insufficiently addressed, particularly regarding the theoretical/computational analysis and the rigor of the proposed SC-ROC mechanism. Therefore, major revision is required before this work can be considered for publication in Nature Communications.
Comments
1 During the OER process, under highly oxidative conditions, the catalyst structure may undergo dynamic structural evolution. It therefore remains unclear whether and how the applied potential and structural reconstruction influence the

proposed SC-ROC mechanism. More direct operando characterization or sufficiently convincing indirect evidence is needed to clarify this point.
2 The authors are encouraged to provide a Pourbaix diagram to identify the thermodynamically stable active phase adopted in the simulations.
3 For the O_2 formation step, both the SC-ROC pathway and the conventional spin-flip mechanism should be systematically investigated and compared in order to validate the claimed superiority of the SC-ROC mechanism in the present work.
4 The computed overpotential is as high as 0.63 V, which deviates significantly from the experimental values. Therefore, a reasonable explanation and/or additional calculations are necessary to reconcile this discrepancy.

Reviewer #3

(Remarks to the Author)
This manuscript presents a strategy for designing an oxygen evolution reaction (OER) electrocatalyst based on a spin-conserved radical oxygen coupling (SC-ROC) mechanism. Starting from a V-doped CoS2 precursor, the authors show that electrochemical oxidation induces selective V leaching, triggering a cascade reconstruction into a coordinatively unsaturated CoOOH (CR-CoOOH). Through operando characterizations (DEMS, Raman, ATR-SEIRAS, XMCD) and DFT calculations, they state that this structural reconfiguration affects Co–O hybridization and enables spin-polarized oxygen-hole states. The study reports a current density of 6.35 A/cm2 at 2.0 V and operation for 2000 hours at 1 A/cm2 in an anion exchange membrane water electrolyzer (AEMWE).

Strengths
1. Catalyst Engineering Strategy: The concept of utilizing selective V-leaching to trigger a cascade reconstruction provides a systematic approach for creating coordinatively unsaturated active sites throughout the catalyst network, as opposed to a typical edge-initiated surface reconstruction.

2. Mechanistic Analysis: The combination of operando isotope-labeled DEMS, XMCD, and spin-polarized DFT calculations provides structural and electronic data for the proposed SC-ROC pathway. It explains the relationship between the spin-polarizable Co–O electronic structure and direct O–O radical coupling.

3. Device-Level Performance: The reported AEMWE performance achieves 6.35 A/cm2 at 2.0 V and maintains 2000 hours of stability at 1 A/cm2, demonstrating the practical viability of the CR-CoOOH catalyst under the tested alkaline conditions.

Weaknesses
1. Discrepancy Regarding Trace Residues: The authors demonstrate that the Co-centered spin signal originates from the cascade reconstruction. However, ICP-OES results (Table S1) indicate that trace amounts of V (0.03 wt%) and S (0.06 wt%) remain in the CR-CoOOH bulk sample, while XPS and EDS (Fig. S3, S9) show no detectable V on the surface. This suggests the trace residues are confined within the bulk. The DFT model of CR-CoOOH (Fig. S38) assumes a pure, dopant-free CoOOH lattice with vacancies. Given that coordinatively unsaturated Co sites are energetically metastable, the potential role of these trace atoms in stabilizing these active defect sites is not addressed in the main text or Supplementary Information.

2. Lack of MEA Post-Mortem Analysis at High Currents: While the study reports stability at high current densities (up to 6 A/cm2), operating at such conditions typically induces mass and heat transport issues that can chemically or mechanically degrade the anion exchange membrane and the catalyst-ionomer interface. Although the structural state of the catalyst itself is analyzed post-operation via XAS (Fig. S32), the structural integrity of the Membrane Electrode Assembly (MEA) cross-section is not investigated.

3. Generality of the Cascade-Reconstruction Strategy: The cascade reconstruction strategy and the SC-ROC mechanism are investigated specifically for the Co-based system. The manuscript lacks data or discussion on whether this design principle can be extended to other conventional OER catalyst systems, such as Ni- or Fe-based materials.

Comments and suggestions
1. Clarification on the Role of Trace Residues: To align the experimental composition with the theoretical model, the authors should clarify the potential stabilizing role of the trace V/S residues. This can be addressed by providing atomic-resolution STEM-EELS mapping to specify the location of the residues, or by adding a DFT discussion on whether a single V/S atom near a vacancy alters the local thermodynamic stability and spin-polarization.

2. Post-Mortem Analysis of the MEA: To verify the device-level durability under high-current AEMWE operations, the authors should provide a post-mortem cross-sectional SEM/EDS analysis of the MEA. Verifying the physical and chemical integrity of the membrane and the catalyst layer interface after the high-current stability test is required.

3. Perspective on Broader Applicability: To evaluate the general applicability of this approach, it would be beneficial to address its universality. We suggest the authors discuss or provide preliminary data on whether this cascade-reconstruction strategy can be extended to other conventional OER catalysts (e.g., V-doped NiS2).

The development of the CR-CoOOH catalyst via a cascade reconstruction strategy provides a functional approach to designing OER electrocatalysts. The operando characterizations and the analysis of the SC-ROC mechanism offer relevant mechanistic data. However, the authors need to address the remaining analytical gaps regarding the exact role of trace

residues in the lattice and the comprehensive MEA structural stability under high-current conditions. We recommend the publication of this manuscript after a Major Revision addressing the comments raised above.

Reviewer #4

(Remarks to the Author)
The manuscript titled “Spin-conserved oxygen-redox coupling enables durable anion exchange membrane water electrolysis” by H. Li et al. reports the synthesis of reconstructed CoOOH with a high density of coordinatively unsaturated Co sites (denoted as CR-CoOOH) and evaluates its electrochemical oxygen evolution reaction (OER) performance. In addition, the authors performed several operando spectroscopic and XMCD measurements to investigate the OER mechanism. Finally, spin-polarized density functional theory (DFT) calculations were carried out to understand the microscopic electronic structure associated with the spin-conserved radical oxygen coupling (SC-ROC) mechanism in CR-CoOOH.

Overall, the authors provide substantial experimental evidence demonstrating that CR-CoOOH exhibits superior OER performance compared to pristine CoOOH and localized reconstructed CoOOH (LR-CoOOH). It is particularly impressive that, beyond the electrochemical measurements, the authors performed state-of-the-art operando spectroscopic studies, which are highly valuable for understanding the OER mechanism. Additionally, the manuscript is generally well written and clearly presented.

However, I find that the XMCD results and their interpretation are not fully convincing. Although the room-temperature magnetic measurements shown in Fig. 2g suggest weak ferromagnetism in CR-CoOOH, the Co L-edge XMCD spectra do not show the typical characteristics of ferromagnetic behavior. In conventional XMCD measurements of ferromagnetic materials, the dichroic signals at the L3 and L2 edges are expected to exhibit opposite signs. However, in Fig. 4f, the XMCD signals at both the L3 and L2 edges appear to have the same sign (positive). The authors should address this point more carefully. Is this behavior related to experimental artifacts (e.g., background subtraction or normalization procedures), or does it originate from intrinsic electronic or magnetic properties of the material? If the latter is the case, the authors should explain why the observed XMCD line shape differs from the commonly reported ferromagnetic XMCD features.

In addition, regarding the XMCD measurements, did the authors apply an external magnetic field to polarize the sample during the measurements? If so, what was the magnitude and direction of the applied magnetic field relative to the sample geometry?

From the perspective of practical device applications, it would also be valuable if the authors could provide further discussion regarding the scalability and stability of CR-CoOOH. Although the material shows superior electrochemical performance, are there any potential concerns regarding the industrial implementation of magnetic CoOOH-based materials, such as safety, stability, or large-scale manufacturability? Furthermore, how stable is the CR-CoOOH phase after synthesis and during long-term storage or operation?

Version 1:

Reviewer comments:

Reviewer #1

(Remarks to the Author)
The author has made revisions, and I believe the current version is acceptable.

Reviewer #2

(Remarks to the Author)
I appreciate the authors' responses to my comments and suggestions. I recommend acceptance of this manuscript for publication. I also suggest uploading the calculation-related coordinate files to the Supporting Information for reproducibility purposes.

Reviewer #3

(Remarks to the Author)
The manuscript has been substantially improved, and the authors have made considerable efforts to address the previous concerns. The responses regarding the role of residual V/S species and the broader applicability of the cascade-reconstruction strategy are satisfactory. However, the concern regarding the structural stability of the membrane electrode assembly under high-current-density operation has not yet been fully addressed.

1. Role of trace V/S residues
The authors have addressed the concern regarding the possible contribution of residual V and S species. The extended ICP-OES analysis, STEM-EDS/EELS characterization, electrochemical control experiments, V/S-containing DFT model,

and EPR characterization of V-doped CoOOH collectively support the conclusion that residual V/S species are not the primary origin of the spin-polarized Co–O electronic structure.
These results also provide a reasonable justification for using a V/S-free reconstructed CoOOH model to represent the dominant active motif of the working catalyst.

2. Post-mortem analysis of the MEA under high-current-density operation
The authors have added cross-sectional and top-view SEM/EDS analyses of an MEA operated at 1 A cm-2 for 100 h. These results show that the catalyst layer and membrane remain physically integrated under this operating condition, without obvious Co migration across the membrane or severe catalyst-layer detachment. However, this experiment does not directly address the original concern regarding MEA stability under high-current-density operation. The manuscript highlights stable operation at 2, 4, and 6 A cm-2 for 100 h at each current density, whereas the post-mortem analysis was performed only after operation at 1 A cm-2 for 100 h. At current densities as high as 6 A cm-2, substantially greater gas evolution, local heating and mechanical stress may be generated within the MEA. These conditions may lead to catalyst-layer cracking, interfacial delamination, membrane deformation, catalyst migration, or local degradation that may not occur at 1 A cm-2.

Therefore, additional post-mortem analysis of an MEA subjected to the reported high-current-density durability test is required. The authors should preferably analyze the MEA used for the sequential durability test at 2, 4, and 6 A cm-2, or alternatively perform a representative durability experiment at 6 A cm-2 followed by post-mortem characterization.
The currently provided 1 A cm-2, 100 h result is useful but cannot substitute for direct post-mortem evaluation under the high-current-density conditions emphasized in the manuscript. This comment therefore remains unresolved and requires additional experimental evidence.

3. Broader applicability of the cascade-reconstruction strategy
The authors have satisfactorily addressed the concern regarding the extension of the cascade-reconstruction strategy beyond the CoOOH system. The newly added CR-NiOOH results demonstrate enhanced OER activity relative to LR-NiOOH and pristine NiOOH. In addition, the isotope-labeling DEMS results provide reasonable preliminary evidence that cascade reconstruction can promote oxygen participation and O–O coupling in a Ni-based oxyhydroxide system. The authors have also appropriately acknowledged that these results do not fully demonstrate spin-conserved radical oxygen coupling in the Ni system and that further spin-sensitive characterization and theoretical analysis would be required. The revised discussion therefore avoids overclaiming the universality of the proposed mechanism.

Overall assessment
The revised manuscript has been significantly strengthened, and two of the three major concerns raised in the previous review have been satisfactorily resolved. Nevertheless, the structural integrity of the MEA under the reported high-current-density operating conditions remains insufficiently verified. Because high-current-density durability is one of the principal practical claims of this work, direct post-mortem characterization of an MEA operated at the reported high current densities is necessary.

Reviewer #4

(Remarks to the Author)
The authors have adequately addressed all of the reviewers' comments and revised the manuscript accordingly. I find the current version of the manuscript satisfactory and recommend that it be accepted for publication in its present form.

Version 2:

Reviewer comments:

Reviewer #3

(Remarks to the Author)
The authors have fully addressed the remainder of our comments and revised the manuscript accordingly. This manuscript should be accepted in Nature Communications without further revision.

Response to referees

We thank the four referees for taking the time to carefully review the manuscript and for giving many useful suggestions. The manuscript has been revised according to their comments and the changes have been highlighted in the revised version. We feel the quality of the paper has been improved greatly thanks to the input from the referees. Below is a point-by-point response.

Reviewer #1 (Remarks to the Author):

This study focuses on the design of cascade-reconstructed CoOOH derived from SC-ROC for high-performance anion exchange membrane water electrolysis. The research idea is clear, the characterization is relatively comprehensive, and the catalytic performance is satisfactory. However, there still exist considerable uncertainties in the experimental setup and mechanism interpretation, which require careful revision and improvement by the authors.

1. In this system, Pt foil is used as the counter electrode in all the three-electrode systems adopted by the author. The oxidation of V-CoS_2 takes as long as 10 hours. Under such prolonged exposure to a strong alkaline environment, trace amounts of Pt may be etched and subsequently deposited and adsorbed onto the surface of the working electrode, thereby leading to an enhancement in catalytic performance. The author is advised to repeat the experiment using a carbon rod or carbon plate as the counter electrode to verify whether the same performance can be achieved.

Response: We thank the reviewer for this comment. We agree that possible Pt-derived contamination from the Pt foil counter electrode should be carefully excluded during prolonged electrochemical reconstruction and OER testing in alkaline electrolyte.

To address this issue, we repeated the electrochemical reconstruction and OER evaluation of CR-CoOOH using a carbon rod as the counter electrode under otherwise identical conditions. After reconstruction, the electrode was thoroughly rinsed and transferred to fresh 1 M KOH electrolyte for OER evaluation, with a carbon rod also used as the counter electrode. As shown in Fig. R1-1, the polarization curve of CR-CoOOH obtained with a carbon rod counter electrode nearly overlaps with that obtained using a Pt foil counter electrode. This result confirms that the high OER activity of CR-CoOOH is reproducible in the absence of a Pt counter electrode, thereby excluding possible Pt-derived contamination from the counter electrode as the origin of the enhanced performance.

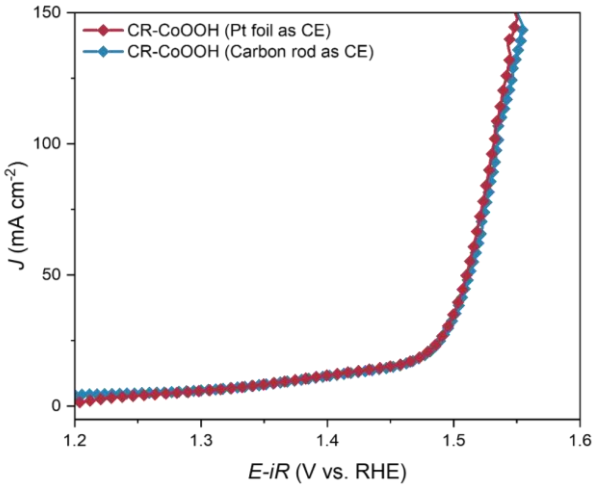

Fig. R1-1 | OER polarization curves of CR-CoOOH reconstructed and evaluated using Pt foil or carbon rod as the counter electrode in 1 M KOH. (Supplementary Fig. 34 in revised manuscript)

To address the comment, we have revised our manuscript as follows

(line 305, page 9, highlighted in yellow): In addition, possible Pt-derived contamination from the Pt foil counter electrode was further excluded by repeating both the electrochemical reconstruction and OER evaluation using a carbon rod counter electrode. The resulting OER polarization curve nearly overlaps with that obtained using the Pt foil counter electrode, confirming that the high OER activity of CR-CoOOH is reproducible in the absence of Pt and does not originate from Pt-derived contamination during prolonged reconstruction or OER testing (Supplementary Fig. 34).

(line 636, page 18, highlighted in yellow): Unless otherwise specified, OER measurements were performed using a Pt foil counter electrode. For the Pt-contamination control experiment, both electrochemical reconstruction and subsequent OER evaluation were repeated using a carbon rod counter electrode under otherwise identical conditions.

2. In this system, the authors confirm that the catalyst simultaneously generates oxygen vacancies and metal defects. Which of these two types of defects plays a dominant role? Could the authors provide experimental evidence to clarify this? Meanwhile, how significantly do different oxidative etching durations affect the catalytic performance? In addition, why did the authors specifically select an etching time of 10 hours?

Response: We thank the reviewer for this important comment. We would first like to clarify the terminology regarding "metal defects". In this work, we did not intend to claim the formation of metal vacancies, such as Co vacancies, in the final CR-CoOOH phase. The "defective" Co sites discussed in the manuscript refer to experimentally observed coordinatively unsaturated Co environments generated by reduced Co–O coordination. Therefore, the active defect motif is more accurately described as oxygen-deficient, coordinatively unsaturated Co–O units generated by Co–O coordination reconfiguration.

Based on our structural and spectroscopic results, the enhanced activity is not dominated by isolated oxygen vacancies or isolated metal defects. Instead, it originates from the coupled Co–O coordination reconfiguration. Co *K*-edge EXAFS fitting shows that the average Co–O coordination number decreases substantially in CR-CoOOH, confirming the formation of abundant coordinatively unsaturated Co–O

environments. Meanwhile, EPR reveals a g ≈ 2.00 signal associated with oxygen-related defect states and a g ≈ 2.16 signal assigned to Co-centered unpaired 3*d* spins. The simultaneous enhancement of these two signals in CR-CoOOH indicates that oxygen-deficient local environments and Co-centered spin polarization are intrinsically coupled within the same reconstructed Co–O motif. Thus, the dominant active motif is the oxygen-deficient, coordinatively unsaturated Co–O unit. This motif generates oxygen-related defect states and perturbs the Co ligand field, making Co-centered unpaired 3*d* spins electronically accessible. These Co-centered unpaired spins can then polarize oxygen-derived hole states through Co–O hybridization and *p–d* exchange, thereby enabling spin-aligned radical O–O coupling.

To evaluate the influence of oxidative etching duration on catalytic performance, we analyzed the chronopotentiometric reconstruction profile at 10 mA cm^{-2}. Since the current density is fixed during this measurement, the recorded potential directly reflects the potential required to sustain 10 mA cm^{-2} at each reconstruction time. As shown in Fig. R1-2, the potential changes markedly during the early stage of oxidative reconstruction, indicating that the catalytic performance is strongly affected by the etching duration before the reconstruction is complete. This evolution is associated with V leaching, sulfur removal, and Co–O coordination reconfiguration (*Energy & Environmental Science 13 (1), 229-237*). After approximately 10 h, the potential reaches a stable plateau, showing that further prolonging the etching time has only a minor influence on the catalytic performance at 10 mA cm^{-2}. Therefore, 10 h was selected as the activation time to ensure that the reconstruction had reached a stable catalytic state.

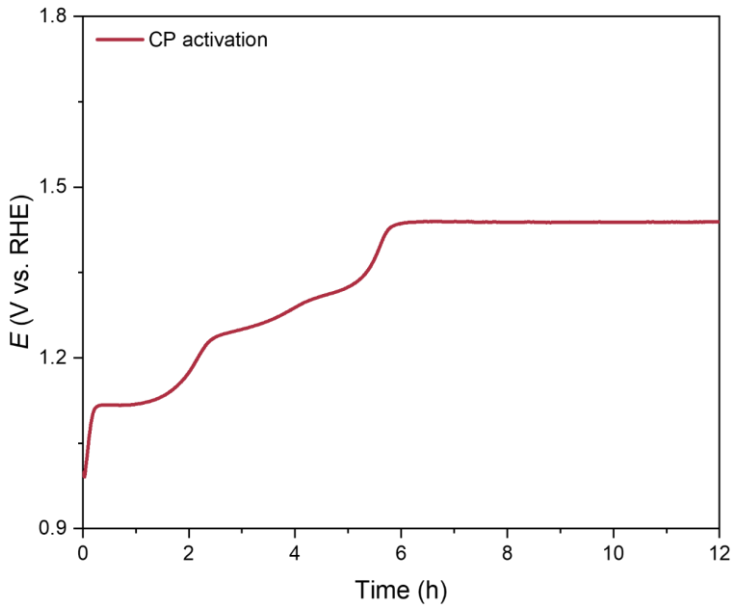

Fig. R1-2 | Chronopotentiometric reconstruction profile of V-CoS_2 at 10 mA cm^{-2}. The potential evolves during oxidative reconstruction and reaches a stable plateau after approximately 10 h, indicating that the reconstructed CR-CoOOH active phase has reached a stable catalytic state. (Supplementary Fig. 5 in revised manuscript)

To address the comment, we have revised our manuscript as follows
(line 132, page 4, highlighted in yellow):
The influence of oxidative reconstruction duration was further evaluated by chronopotentiometry at 10 mA cm^{-2}. The potential changes markedly during the early reconstruction stage and then reaches a stable plateau, indicating that the reconstructed catalyst has reached a stable catalytic state (Supplementary Fig.5).

Therefore, 10 h was selected as the activation time to ensure complete and stable reconstruction after the plateau was reached.

(line 257, page 8, highlighted in yellow): Overall, these results identify oxygen-deficient, coordinatively unsaturated Co–O units as the dominant active motif in CR-CoOOH, rather than isolated oxygen vacancies or metal-defect sites. The cascade reconstruction induced Co–O coordination reconfiguration creates oxygen-related defect states and induces a high density of exchange-correlated unpaired spins within the reconstructed Co–O network, thereby providing the magnetic foundation for spin-polarized oxygen redox.

(line 602, page 17, highlighted in yellow):

A constant current density of 10 mA cm^{-2} was applied to V-doped CoS_2/CC for 10 h to obtain a stable reconstructed oxyhydroxide phase, denoted as CR-CoOOH.

3. The conclusion emphasizes that SC-ROC is a universal design principle, but it has only been validated in a Co-based system. Please briefly discuss the applicability of this strategy to other transition metal systems (e.g., Ni, Fe) to strengthen the scientific significance.

Response: We thank the reviewer for this constructive suggestion. We agree that, because the main experimental validation in the original manuscript was performed on a Co-based reconstructed oxyhydroxide, the universality of SC-ROC should not be overclaimed. We have therefore revised the wording in the conclusion from a "universal" design principle to a "potentially generalizable" strategy, and added a discussion on its applicability to other transition-metal oxyhydroxides.

From an electronic-structure perspective, the proposed strategy may be extendable to other transition-metal oxyhydroxides (MOOH) beyond CoOOH if the MOOH can simultaneously provide oxygen-hole formation, spin-active metal 3*d* states, and adjacent oxygen-coupling geometry. We selected CoOOH as the main model system because conventional CoOOH is dominated by weakly hybridized t_{2g}–O 2*p*π interactions, which suppress oxygen-hole formation and provide negligible Co-centered unpaired spins. Therefore, the reconstruction-induced transition from a weakly hybridized, spin-inactive Co–O framework to a *σ*-type e_g–O 2*p* hybridized and spin-polarizable Co–O framework provides a clear platform to demonstrate the SC-ROC design principle.

For Ni-based oxyhydroxides, coordinatively unsaturated Ni–O units may also provide electronically favorable motifs for O–O coupling. From a ligand-field perspective, reducing the Ni–O coordination can lower the local symmetry of NiO_{6-x} units and perturb the splitting and occupancy of Ni e_g-derived states, which are directly involved in *σ*-type Ni e_g–O 2*p* hybridization. Such perturbation may facilitate the participation of O 2*p*-derived ligand-hole states in oxygen redox. More importantly, when these oxygen-derived hole states are coupled with partially occupied Ni e_g-derived states through Ni–O covalency, *p*–*d* exchange interactions may provide a possible route for spin polarization of oxygen-centered radicals. Therefore, coordinatively unsaturated Ni–O units are, in principle, plausible motifs for activating oxygen-redox/radical O–O coupling.

To provide preliminary proof-of-concept evidence that this strategy is extendable to Ni-based oxyhydroxides, we further constructed a Ni-based analogue by reconstructing V-NiS_2 into CR-NiOOH. As shown in Fig. R1-3, CR-NiOOH exhibits enhanced OER activity compared with LR-NiOOH and pristine NiOOH. Moreover, isotope-labeling DEMS shows a pronounced m/z = 36 signal for ^{18}O-labeled CR-NiOOH, whereas ^{18}O-labeled NiOOH shows negligible m/z = 36 response (Fig. R1-4). These results indicate that

cascade reconstruction can also activate oxygen participation and O–O coupling in a NiOOH-based system. We note that this Ni-based experiment serves as a preliminary proof-of-concept for the broader applicability of the reconstruction-enabled oxygen-redox strategy, while full validation of spin-conserved coupling in non-Co systems would require further spin-sensitive characterizations.

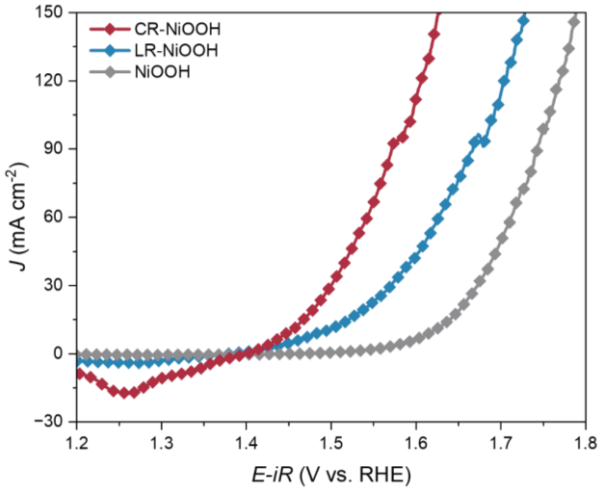

Fig. R1-3 | LSV curves of CR-NiOOH, LR-NiOOH, and NiOOH in fresh 1 M KOH. (Supplementary Fig. 50 in revised manuscript)

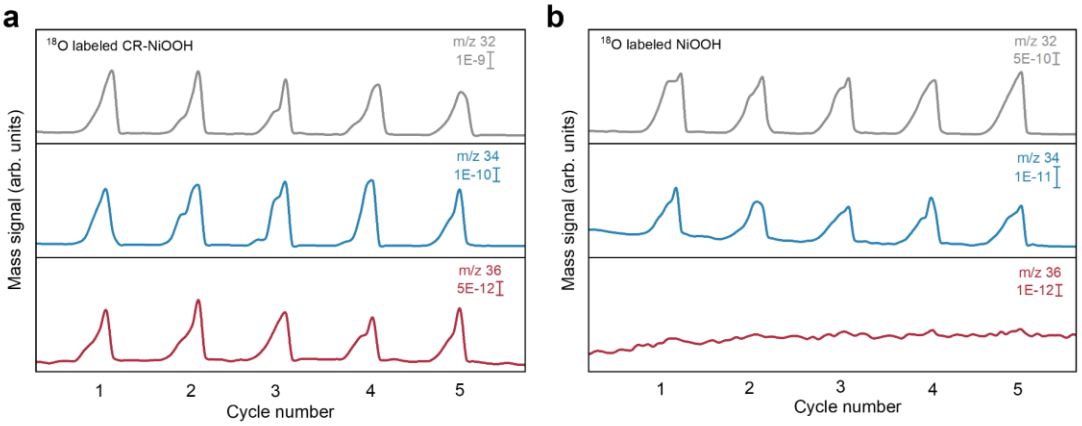

Fig. R1-4 | Operando DEMS characterization. a Operando DEMS signals of O_2 products for ^{18}O-labeled CR-NiOOH. **b** Operando DEMS signals of O_2 products for ^{18}O-labeled NiOOH. (Supplementary Fig. 51 in revised manuscript)

For Fe-based oxyhydroxides, the applicability of this strategy can be considered from the same three requirements: oxygen-hole formation, spin-active metal–oxygen states, and adjacent oxygen-coupling geometry. Fe centers, especially Fe^{3+} with a $3d^5$ configuration, can in principle provide spin-active 3*d* states because of the presence of unpaired 3*d* electrons. If coordinatively unsaturated Fe–O units can be engineered to promote oxygen-hole formation and suitable Fe 3*d*–O 2*p* coupling, such spin-active Fe states may provide a possible exchange channel for polarizing oxygen-derived intermediates. Therefore, Fe-based oxyhydroxides may also be considered potential candidates for SC-ROC-type oxygen-redox coupling, which requires independent experimental and theoretical validation.

To address the comment, we have revised our manuscript as follows (line 555, page 16, highlighted in yellow): Although this work focuses on a Co-based reconstructed oxyhydroxide, the underlying design concept may be extendable to other transition-metal oxyhydroxides if the reconstructed MOOH phase can provide oxygen-hole formation, spin-active metal 3*d* states, and adjacent oxygen-coupling geometry. For Ni-based oxyhydroxides, coordinatively unsaturated Ni–O units may perturb the local ligand field and modulate Ni e_g–O 2*p* hybridization, thereby facilitating oxygen-redox participation and radical O–O coupling. As preliminary proof-of-concept evidence, we constructed a Ni-based analogue by reconstructing V-NiS_2 into CR-NiOOH. CR-NiOOH exhibits enhanced OER activity compared with LR-NiOOH and pristine NiOOH (Supplementary Fig. 50). Isotope-labeling DEMS shows a pronounced m/z = 36 signal for ^{18}O-labeled CR-NiOOH, whereas ^{18}O-labeled NiOOH shows negligible response, indicating reconstruction-enabled oxygen participation and O–O coupling in a NiOOH-based system (Supplementary Fig. 51). For Fe-based oxyhydroxides, spin-active Fe 3*d* states may also provide a possible exchange channel for polarizing oxygen-derived intermediates if suitable Fe–O coordination and oxygen-hole states can be engineered. Nevertheless, full validation of SC-ROC in non-Co systems requires further spin-sensitive characterization and theoretical analysis.

Overall, the spin-regulated oxygen redox mechanism demonstrated in CR-CoOOH underpins its exceptional activity and durability in AEMWE. More broadly, these findings highlight spin-selective electronic structure and *p*–*d* exchange within reconstructed metal–oxygen units as powerful yet underexplored design parameters for advancing oxygen evolution catalysis and other multielectron redox reactions.

4. Please supplement a comprehensive comparison of the OER performance (overpotential and Tafel slope) of this catalyst with state-of-the-art OER catalysts reported in recent literature.

Response: We thank the reviewer for this constructive suggestion. Following the reviewer's advice, we have supplemented a comprehensive comparison of the OER performance of CR-CoOOH with recently reported state-of-the-art OER electrocatalysts. As shown in Fig. R1-5, the comparison includes both the overpotential required to reach 10 mA cm^{-2} and the corresponding Tafel slope. CR-CoOOH exhibits a low overpotential of 185 mV at 10 mA cm^{-2} and a Tafel slope of 58 mV dec^{-1}, placing it in the low-overpotential/low-Tafel-slope region among the compared catalysts. This comparison further highlights the favorable OER kinetics and competitive activity of CR-CoOOH.

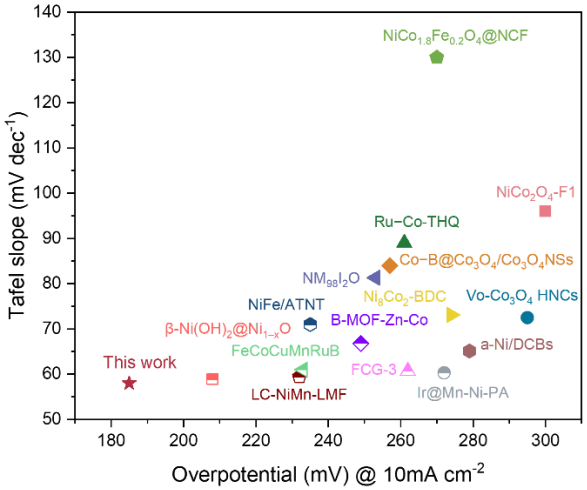

Fig. R1-5 | Scatter plot comparing the overpotential at 10 mA cm^{-2} and Tafel slope of CR-CoOOH with representative OER catalysts reported in recent literature from Supplementary Table 3 (Supplementary Fig.

29 in revised manuscript).

To address the comment, we have revised our manuscript as follows (line 284, page 9, highlighted in yellow): Compared with recently reported state-of-the-art OER electrocatalysts, CR-CoOOH shows a competitive combination of low overpotential at 10 mA cm^{-2} and small Tafel slope (Supplementary Fig. 29 and Supplementary Table 3), further highlighting its strong OER performance.

5. For the as-prepared CR-CoOOH catalyst, the influence of the vanadium component cannot be ruled out, and the contribution of trace vanadium to the catalytic performance needs to be evaluated. Moreover, the theoretical calculation model established by the authors also fails to take the effect of V into account.

Response: We thank the reviewer for raising this important point. We agree that the possible contribution of residual V species should be carefully evaluated. In our design, V acts as a sacrificial dopant to trigger cascade reconstruction, rather than as the final catalytic active component. During electrochemical reconstruction, V species are preferentially leached into the electrolyte, accompanied by sulfur oxidation and reorganization of the Co–O local environment. The time-dependent XPS and ICP analyses show the near-complete removal of V and S species after reconstruction (Fig. R1-6 and Table R1-1).

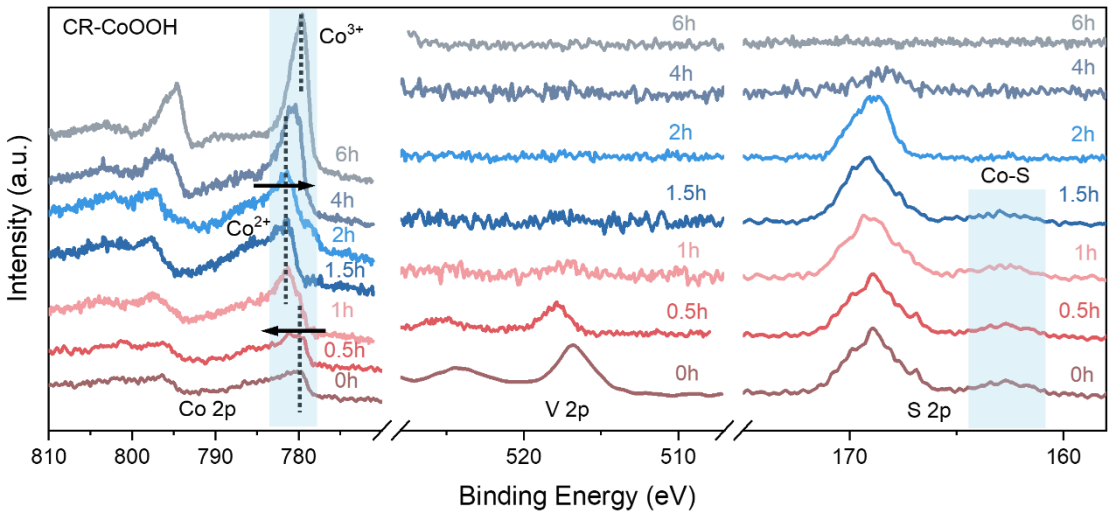

Fig. R1-6 | High-resolution Co 2*p*, V 2*p*, and S 2*p* XPS spectra of CR-CoOOH recorded after different electrochemical activation times (0-6 h). (Supplementary Fig. 4 in revised manuscript)

Table R1-1 | ICP analysis of V–CoS2 after activation for different durations (Supplementary Table. 1 in revised manuscript)

$V\text{-}CoS_2$ Stage	Mass ratio of Co (wt%)	Mass ratio of S (wt%)	Mass ratio of V (wt%)
0 h	37.92	27.63	3.02
2 h	20.28	0.28	0.25
4 h	20.03	0.23	0.19
6h	19.96	0.06	0.03
10 h	21.55	N/A	N/A

To further evaluate the possible contribution of trace V-derived species, we performed additional control experiments. First, after electrochemical reconstruction, the CR-CoOOH electrode was thoroughly rinsed and transferred to fresh 1 M KOH for OER evaluation (Fig.R1-7). The polarization curve remained nearly unchanged compared with that measured before electrolyte replacement, confirming that soluble species generated during reconstruction do not account for the enhanced activity. Second, we deliberately added vanadate and sulfate ions into fresh 1 M KOH and measured the OER performance of CR-CoOOH. The addition of these ions caused negligible changes in the OER polarization curves. These results demonstrate that trace vanadate/sulfate species in the electrolyte do not provide a measurable catalytic enhancement.

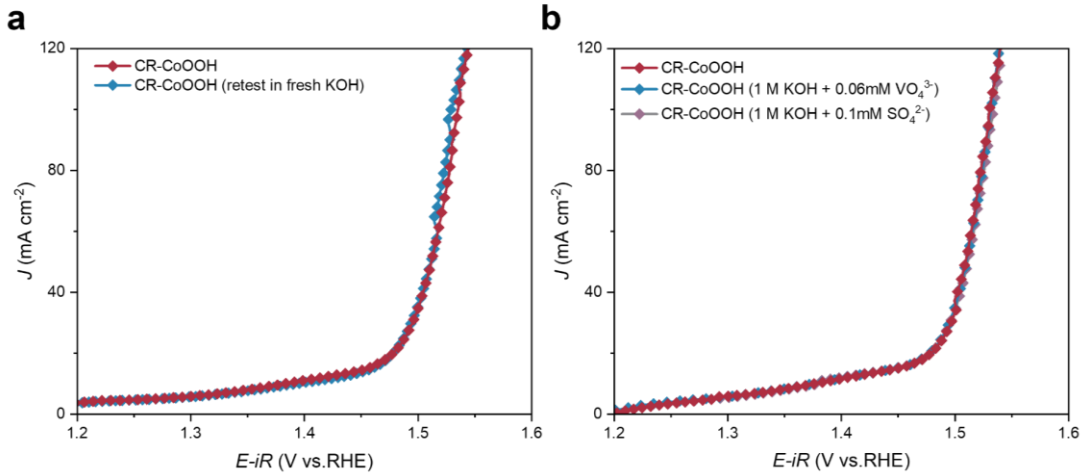

Fig. R1-7 | Control experiments excluding the activity contribution of soluble or weakly adsorbed V/S-derived species. a, OER polarization curves of CR-CoOOH measured before and after transferring the reconstructed electrode into fresh 1 M KOH. **b,** OER polarization curves of CR-CoOOH measured in fresh 1 M KOH with and without deliberately added vanadate and sulfate ions. (Supplementary Fig. 33 in revised manuscript)

We further examined whether V incorporation itself can generate the spin-polarizable Co–O electronic structure required for SC-ROC (Fig. R1-8). As an additional control, V-doped CoOOH was prepared and characterized by EPR. No detectable Co-centered unpaired-spin signal at g = 2.16 was observed for V-CoOOH, in contrast to the pronounced signal in CR-CoOOH. This result indicates that conventional V incorporation and leaching alone cannot produce the exchange-correlated Co-centered unpaired spins observed in CR-CoOOH.

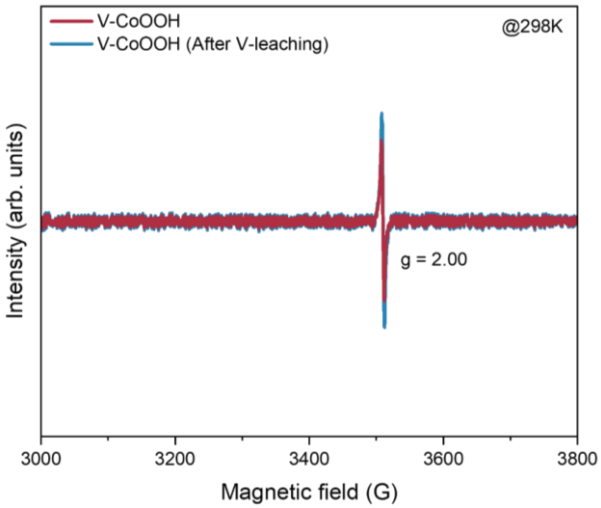

Fig. R1-8 | EPR characterization on V-CoOOH before and after electrochemical V-leaching. (Supplementary Fig. 22a in revised manuscript)

Consistently, our additional DFT calculations on V-CoOOH do not reproduce the spin-polarized Co–O electronic structure characteristic of CR-CoOOH (Fig. R1-9). The calculated spin-density distribution is mainly localized around V-related sites and does not generate the exchange-correlated Co–O spin polarization required for SC-ROC. Therefore, the key factor is not residual V doping, but the V-leaching-triggered cascade reconstruction that generates oxygen-deficient, coordinatively unsaturated Co–O units.

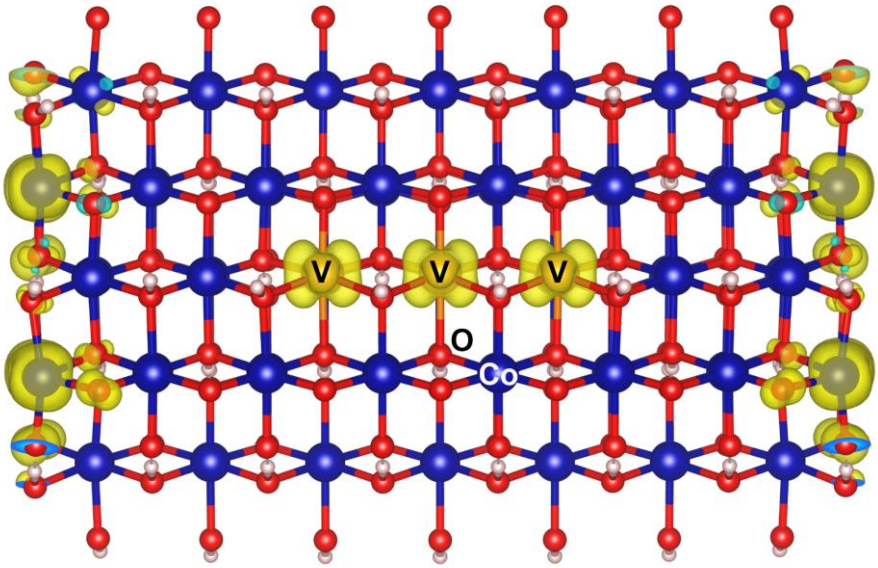

Fig. R1-9 | Spin-density isosurface of V-CoOOH. (Supplementary Fig. 48 in revised manuscript)

Based on these results, the DFT model without V is appropriate for describing the final reconstructed active phase. Since V is removed during reconstruction and does not reproduce the spin-polarizable Co–O electronic structure when retained as a dopant, including V in the main CR-CoOOH model would not represent the experimentally identified active phase.

To address the comment, we have revised our manuscript as follows

(line 141, page 4, highlighted in yellow): To further quantify the compositional evolution, time-dependent ICP analysis was conducted after prolonged electrochemical reconstruction. After 10 h activation, both V and S become undetectable within the detection limits (Supplementary Table 1), further confirming that these elements are not retained as stable components in the reconstructed catalyst. This compositional evolution supports that V and S primarily participate in triggering the reconstruction process, rather than serving as final catalytic active components.

(line 234, page 7, highlighted in yellow): In particular, V–CoOOH does not show the characteristic $g \approx 2.16$ signal even after electrochemical V leaching, further excluding residual V incorporation as the origin of the spin-polarizable Co–O electronic structure.

(line 510, page 15, highlighted in yellow): Second, a V-doped CoOOH model was calculated to examine whether V incorporation itself can generate Co–O spin polarization. The V-doped CoOOH model does not reproduce the extended spin-polarized Co–O electronic structure observed in CR-CoOOH (Supplementary Fig. 48). These results indicate that the spin-polarizable Co–O electronic structure required for SC-ROC originates primarily from cascade-reconstruction-induced Co–O coordination reconfiguration, rather than from residual V/S species or simple V incorporation.

6. The precursors of CR-CoOOH and LR-CoOOH (i.e., V-CoS_2 and CoS_2) exhibit obvious differences in microstructure and XPS peak profiles. It is necessary to clarify whether such differences serve as a key factor leading to the performance discrepancy of the derived catalysts.

Response: We thank the reviewer for this insightful comment. We agree that the V-CoS_2 and CoS_2 precursors exhibit noticeable differences in microstructure and surface XPS features. These differences are expected, as V incorporation can modify the local chemical environment, surface oxidation state, and microstructure of the sulfide precursor. However, the pristine precursors are not the catalytically relevant phases under OER conditions. Both V-CoS_2 and CoS_2 undergo electrochemical reconstruction before OER evaluation, yielding CR-CoOOH and LR-CoOOH, respectively. Therefore, the performance discrepancy should be evaluated based on the reconstructed oxyhydroxide active phases.

For V-CoS_2, the incorporation and subsequent leaching of V serves as a sacrificial trigger for cascade reconstruction, accompanied by sulfur oxidation and Co–O coordination reconfiguration, ultimately producing CR-CoOOH. In contrast, CoS_2 is reconstructed into LR-CoOOH under the same activation conditions. After reconstruction, CR-CoOOH and LR-CoOOH show clear differences in their local coordination and electronic structures (Fig. R1-10). Co *K*-edge EXAFS indicates that CR-CoOOH has a much lower average Co–O coordination number than LR-CoOOH, indicating more abundant coordinatively unsaturated Co–O units. O *K*-edge XAS further reveals stronger Co–O hybridization in CR-CoOOH, while EPR and magnetic measurements show more pronounced Co-centered unpaired spins and exchange-correlated magnetic behavior. These post-reconstruction features directly correlate with the enhanced OER activity and the proposed SC-ROC mechanism.

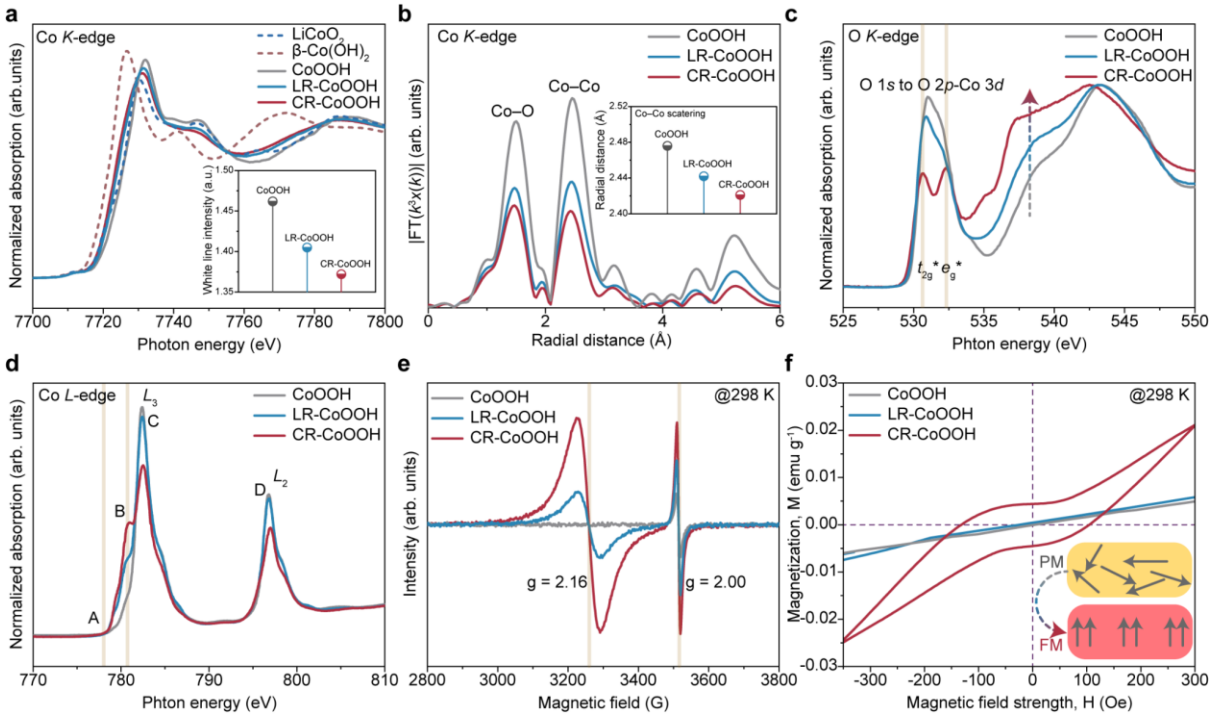

Fig. R1-10 | Structural characterization of CR-CoOOH. a Co *K*-edge XAS spectra of CoOOH, LR-CoOOH, and CR-CoOOH, with $LiCoO_2$ and β-$Co(OH)_2$ as references. **b** Fourier-transforms of k^3-weighted Co *K*-edge EXAFS spectra of CoOOH, LR-CoOOH, and CR-CoOOH. **c** O *K*-edge XAS spectra of CoOOH, LR-CoOOH, and CR-CoOOH. **d** Co *L*-edge XAS spectra of CoOOH, LR-CoOOH, and CR-CoOOH. **e** EPR spectra of CoOOH, LR-CoOOH, and CR-CoOOH. **f** Magnetic hysteresis loop of CoOOH, LR-CoOOH, and CR-CoOOH. (Fig. 1 b-g in revised manuscript)

We also considered the possible influence of precursor morphology on the apparent activity. The microstructural differences of the pristine precursors may affect the electrochemically accessible surface area of the active phase; however, the ECSA-normalized activity of CR-CoOOH remains substantially higher than that of LR-CoOOH and CoOOH (Fig. R1-11). This confirms that the activity enhancement cannot be simply attributed to precursor morphology or surface area differences. Therefore, while the precursor differences influence how the reconstructed oxyhydroxide phase is formed, the key factor determining the final intrinsic OER performance is the reconstructed CR-CoOOH active phase with coordination-reconfigured, spin-polarizable Co–O units.

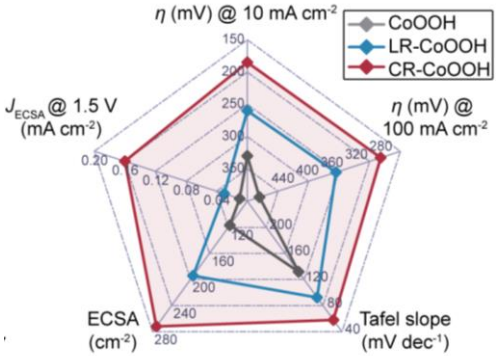

Fig. R1-11 | Radar chart summarizing key electrochemical parameters for CR-CoOOH, LR-CoOOH, and

CoOOH. (Fig. 3b in revised manuscript)

To address the comment, we have revised our manuscript as follows

(Supplementary Fig. 17, highlighted in yellow): Although V-CoS_2 and CoS_2 show differences in precursor morphology and surface XPS features, these pristine sulfide precursors are not the final catalytically active phases under OER conditions. Both precursors undergo electrochemical reconstruction into oxyhydroxide active phases before OER evaluation, yielding CR-CoOOH and LR-CoOOH, respectively. Therefore, the performance difference between CR-CoOOH and LR-CoOOH should be evaluated primarily based on the reconstructed oxyhydroxide phases rather than the pristine sulfide precursors.

(line 293, page 9, highlighted in yellow): The higher ECSA-normalized activity of CR-CoOOH further indicates that its enhanced OER performance cannot be simply attributed to precursor morphology or surface-area differences, but arises from the intrinsically improved activity of the reconstructed CR-CoOOH phase.

Reviewer #2 (Remarks to the Author):

Li and coauthors reported a cascade-reconstructed CoOOH (CR-CoOOH) catalyst that enables a spin-conserved radical oxygen coupling (SC-ROC) pathway for the oxygen evolution reaction (OER). By combining operando spectroscopy, magnetic characterization, isotope-labeled DEMS, and electrochemical measurements, the authors provide a relatively comprehensive dataset supporting the involvement of oxygen-redox chemistry. In addition, the work demonstrates impressive device-level performance. Overall, the manuscript is of considerable interest. However, several important issues remain insufficiently addressed, particularly regarding the theoretical/computational analysis and the rigor of the proposed SC-ROC mechanism. Therefore, major revision is required before this work can be considered for publication in Nature Communications.

Comments:

1 During the OER process, under highly oxidative conditions, the catalyst structure may undergo dynamic structural evolution. It therefore remains unclear whether and how the applied potential and structural reconstruction influence the proposed SC-ROC mechanism. More direct operando characterization or sufficiently convincing indirect evidence is needed to clarify this point.

Response: We thank the reviewer for this insightful comment. In our system, cascade reconstruction first converts the V-CoS_2 into the CR-CoOOH active phase. This reconstructed phase provides coordinatively unsaturated Co–O units, enhanced Co–O hybridization, and spin-polarizable Co–O electronic states. The applied anodic potential then activates this reconstructed active phase by generating oxygen-redox and radical oxygen-coupling intermediates required for SC-ROC.

To clarify this point, we have added a quantitative analysis of the potential-dependent operando Raman and ATR-SEIRAS results. As shown in Fig. R2-1a, when the applied potential enters the OER-relevant region, the normalized intensity of the Raman signal assigned to O–O species increases markedly. Similarly, the normalized intensity of the ATR-SEIRAS O–O band progressively increases with applied potential (Fig. R2-1b). These potential-dependent operando vibrational results directly show that O–O coupling intermediates are generated and enhanced under anodic OER potentials, supporting the potential-activated nature of the proposed SC-ROC mechanism. This conclusion is further supported by the isotope-labeling DEMS results, which confirm oxygen participation in O–O bond formation during OER, and by the methanol probe experiment, which indicates the involvement of reactive oxygen species on CR-CoOOH.

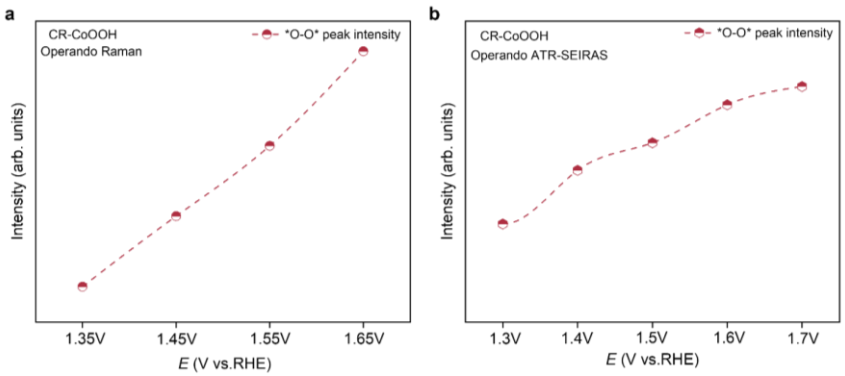

Fig. R2-1 | Potential-dependent evolution of O–O-related vibrational bands under OER conditions. (Supplementary Fig. 42 in revised manuscript)

In addition, post-stability Co *K*-edge XAS/EXAFS shows negligible changes after high-current operation, indicating that the reconstructed CR-CoOOH active phase is largely preserved during OER (Fig. R2-2). Therefore, the working-state evolution mainly corresponds to potential-induced formation of reactive O–O coupling intermediates within a stable reconstructed CR-CoOOH phase, rather than continuous irreversible reconstruction into a different catalyst.

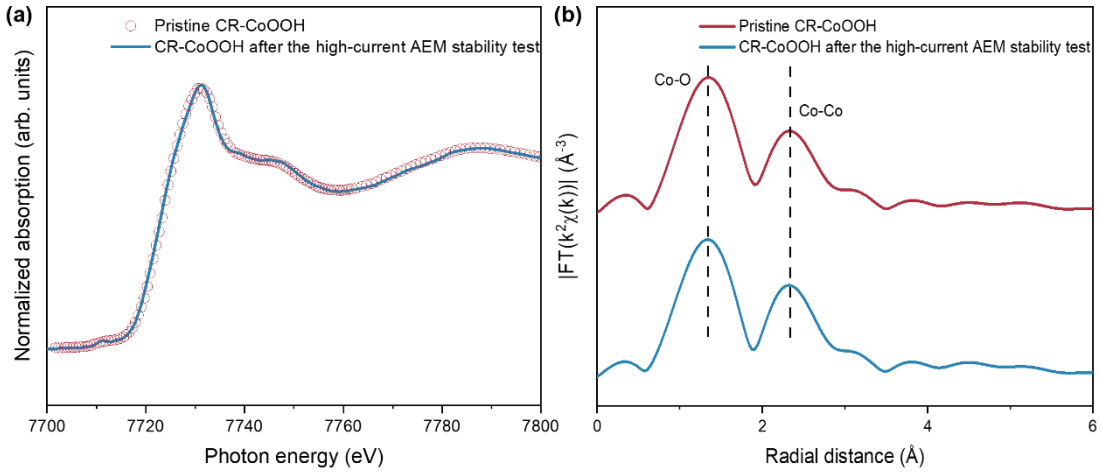

Fig. R2-2 | Structural stability of CR-CoOOH after high-current AEMWE operation. **a**, Co *K*-edge XANES spectra of CR-CoOOH collected before and after 300 h durability testing in an AEM electrolyzer at 2, 4, and 6 A cm^{-2}. **b**, Fourier-transformed EXAFS spectra showing negligible changes in the local coordination environment. (Supplementary Fig. 36 in revised manuscript)

To address the comment, we have revised our manuscript as follows

(line 412, page 12, highlighted in yellow): Quantitative analysis of the potential-dependent Raman spectra shows that when the applied potential enters the OER-relevant region, the normalized intensity of this O–O-related Raman band increases markedly (Supplementary Fig. 42a). Similarly, the normalized intensity of the O–O-related band in operando ATR-SEIRAS progressively increases with applied potential (Supplementary Fig. 42b). These potential-dependent vibrational results indicate that O–O coupling intermediates are generated and enhanced under anodic OER potentials.

(line 334, page 10, highlighted in yellow): This structural retention indicates that CR-CoOOH remains largely preserved during operation, excluding continuous irreversible transformation into a different cobalt phase under high-current OER conditions.

2 The authors are encouraged to provide a Pourbaix diagram to identify the thermodynamically stable active phase adopted in the simulations.

Response: We thank the reviewer for this helpful suggestion. Following the reviewer's advice, we have added a Pourbaix-diagram analysis to identify the thermodynamically stable cobalt phase under alkaline OER conditions and to justify the active phase adopted in the DFT simulations.

As shown in Fig. R2-3, under the alkaline and anodic potential region relevant to OER, the thermodynamically stable cobalt-containing solid phase is $CoHO_2(s)$, corresponding to a oxyhydroxide phase. In contrast, the sulfide-derived S species are not thermodynamically stable as lattice sulfide under

these oxidative conditions and are expected to be oxidized into soluble sulfate species. This result supports the electrochemical reconstruction of the sulfide precursor into a CoOOH-type active phase during OER operation.

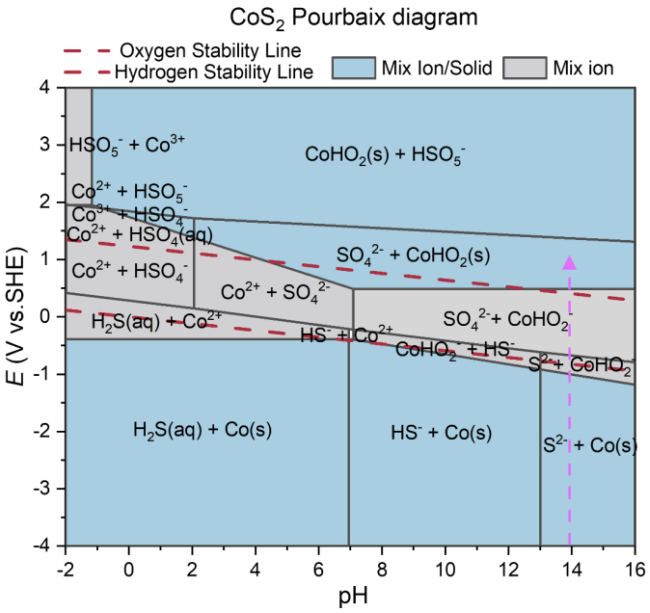

Fig. R2-3 | Pourbaix-diagram analysis of the thermodynamically stable phase under alkaline OER conditions**.** (Supplementary Fig. 45 in revised manuscript)

Therefore, the reconstructed CoOOH phase, rather than the initial sulfide precursor or a sulfur-retaining phase, was used as the active phase model in the DFT calculations. This assignment is also consistent with the post-reconstruction compositional characterization. In particular, V and S are progressively removed during electrochemical reconstruction and become undetectable after prolonged activation, indicating that they do not remain as stable components in the final reconstructed catalyst (Fig. R2-4).

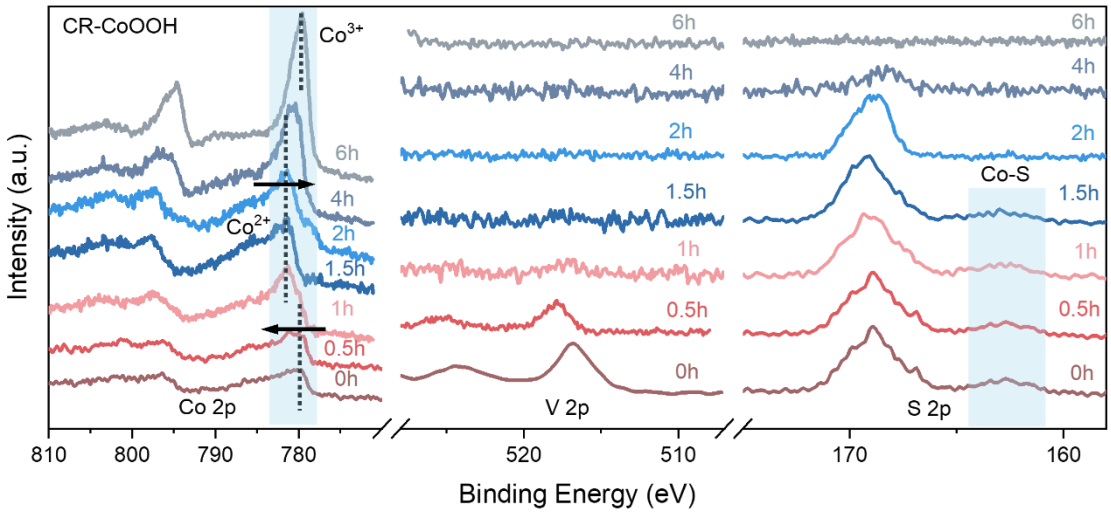

Fig. R2-4 | High-resolution Co 2*p*, V 2*p*, and S 2*p* XPS spectra of CR-CoOOH recorded after different electrochemical activation times (0-6 h). (Supplementary Fig. 4 in revised manuscript)

To address the comment, we have revised our manuscript as follows (line 446, page 13, highlighted in yellow): This model choice is also supported by the CoS_2 Pourbaix-diagram analysis, which shows that under alkaline anodic OER conditions the thermodynamically stable cobalt-containing solid phase is $CoHO_2$(s), corresponding to a CoOOH-like oxyhydroxide phase (Supplementary Fig.45).

3 For the O_2 formation step, both the SC-ROC pathway and the conventional spin-flip mechanism should be systematically investigated and compared in order to validate the claimed superiority of the SC-ROC mechanism in the present work.

Response: We thank the reviewer for this important suggestion. Following the reviewer's advice, we further compared the energetic preference for forming spin-aligned and spin-inverse oxygen-radical configurations involved in the O_2 formation process on CR-CoOOH.

As shown in Fig. R2-5, the calculated formation energy of the spin-aligned oxygen-radical configuration is 0.39 eV, whereas that of the spin-inverse configuration is 0.90 eV. Therefore, the spin-aligned configuration is thermodynamically more favorable by 0.51 eV. This result indicates that maintaining the spin alignment of oxygen-radical intermediates stabilizes the O–O coupling configuration and lowers the energetic requirement for forming the key oxygen-coupling state. This supports the thermodynamic preference of the SC-ROC pathway over the spin-inverse oxygen-coupling configuration. Rather than relying only on the overall OER free-energy diagram, this additional spin-configuration comparison directly shows that the spin-conserved arrangement is energetically favored during the oxygen-coupling process.

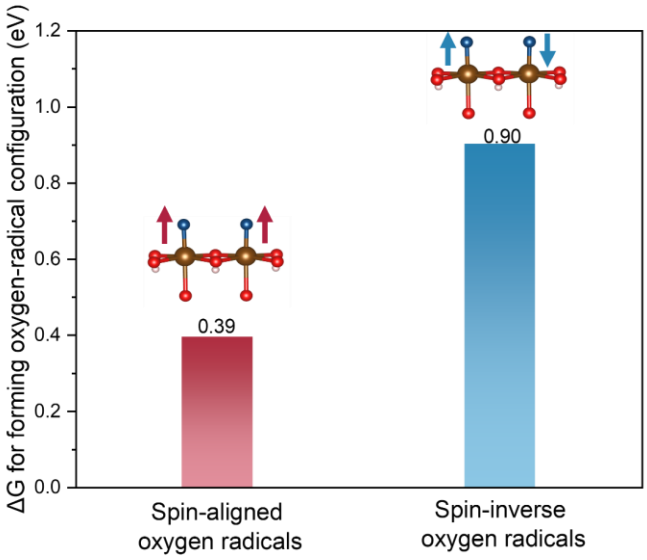

Fig. R2-5 | Calculated formation energies of spin-aligned and spin-inverse oxygen-radical configurations involved in the O_2 formation process on CR-CoOOH. (Supplementary Fig. 49 in revised manuscript)

To address the comment, we have revised our manuscript as follows (line 525, page 15, highlighted in yellow): To further compare the oxygen-coupling configurations with different spin arrangements, we calculated the formation energies of spin-aligned and spin-inverse oxygen-radical configurations involved in the O_2 formation process. The spin-aligned configuration shows a lower formation energy of 0.39 eV, whereas the spin-inverse configuration requires 0.90 eV (Supplementary Fig. 49). This comparison indicates that maintaining spin alignment stabilizes the oxygen-coupling configuration and makes the spin-conserved

arrangement thermodynamically more favorable than the spin-inverse configuration. These free-energy and spin-configuration comparisons provide theoretical support for the experimentally observed preference for radical O–O coupling on CR-CoOOH.

4 The computed overpotential is as high as 0.63 V, which deviates significantly from the experimental values. Therefore, a reasonable explanation and/or additional calculations are necessary to reconcile this discrepancy.
Response: We thank the reviewer for pointing out this issue. We would like to clarify that the computed value of 0.63 V and the experimentally measured overpotential at 10 mA cm^{-2} describe different levels of catalytic behavior and therefore should not be directly compared on a one-to-one basis. The calculated value is derived from Gibbs free-energy differences within the computational hydrogen electrode framework for an idealized local active-site model, and serves as a thermodynamic descriptor for comparing reaction pathways. In contrast, the experimental η_{10} is an apparent electrode-level metric determined by both intrinsic site energetics and extrinsic factors, including active-site density, ECSA, electrode morphology, conductivity, mass transport, bubble release, electrolyte environment, and *iR* correction.

In this work, the purpose of the DFT calculation is to compare the relative thermodynamic feasibility of the SC-ROC and conventional AEM pathways under the same computational framework, rather than to quantitatively predict the experimental overpotential. Importantly, the limiting free-energy requirement of the SC-ROC pathway is lower than that of the conventional AEM pathway, indicating that the spin-conserved radical oxygen-coupling route is thermodynamically more favorable on the reconstructed CR-CoOOH active phase.

Further, we would like to clarify that the proposed SC-ROC mechanism is not based solely on the DFT-derived value. The DFT results are used as supportive evidence to rationalize the experimentally observed pathway preference from the electronic-structure perspective. The main mechanistic evidence comes from isotope-labeling DEMS, potential-dependent operando Raman/ATR-SEIRAS, and chemical-probe experiments, which directly indicate oxygen participation and O–O coupling under OER conditions. Therefore, the calculated 0.63 V should be interpreted as qualitative thermodynamic support for the experimentally identified SC-ROC pathway, rather than as a standalone quantitative prediction of the catalytic overpotential.

To address the comment, we have revised our manuscript as follows (line 518, page15, highlighted in yellow):
For the conventional AEM, the limiting free-energy requirement is 0.74 eV. In contrast, the SC-ROC pathway on CR-CoOOH exhibits a lower limiting free-energy requirement of 0.63 eV, indicating that the spin-aligned radical oxygen-coupling process is thermodynamically more accessible. It should be noted that this DFT-derived value is a thermodynamic descriptor obtained from Gibbs free-energy differences for an idealized local active-site model, rather than a direct prediction of the experimental overpotential at 10 mA cm^{-2}. This difference arises because the DFT value reflects the thermodynamic requirement of an idealized local site, whereas the experimental overpotential is an electrode-level metric affected by active-site density, ECSA, transport, conductivity, and *iR*-correction.

Reviewer #3 (Remarks to the Author):

This manuscript presents a strategy for designing an oxygen evolution reaction (OER) electrocatalyst based on a spin-conserved radical oxygen coupling (SC-ROC) mechanism. Starting from a V-doped CoS_2 precursor, the authors show that electrochemical oxidation induces selective V leaching, triggering a cascade reconstruction into a coordinatively unsaturated CoOOH (CR-CoOOH). Through operando characterizations (DEMS, Raman, ATR-SEIRAS, XMCD) and DFT calculations, they state that this structural reconfiguration affects Co–O hybridization and enables spin-polarized oxygen-hole states. The study reports a current density of 6.35 A/cm^2 at 2.0 V and operation for 2000 hours at 1 A/cm^2 in an anion exchange membrane water electrolyzer (AEMWE).

Strengths

1. Catalyst Engineering Strategy: The concept of utilizing selective V-leaching to trigger a cascade reconstruction provides a systematic approach for creating coordinatively unsaturated active sites throughout the catalyst network, as opposed to a typical edge-initiated surface reconstruction.

2. Mechanistic Analysis: The combination of operando isotope-labeled DEMS, XMCD, and spin-polarized DFT calculations provides structural and electronic data for the proposed SC-ROC pathway. It explains the relationship between the spin-polarizable Co–O electronic structure and direct O–O radical coupling.

3. Device-Level Performance: The reported AEMWE performance achieves 6.35 A/cm^2 at 2.0 V and maintains 2000 hours of stability at 1 A/cm2, demonstrating the practical viability of the CR-CoOOH catalyst under the tested alkaline conditions.

Weaknesses

1. Discrepancy Regarding Trace Residues: The authors demonstrate that the Co-centered spin signal originates from the cascade reconstruction. However, ICP-OES results (Table S1) indicate that trace amounts of V (0.03 wt%) and S (0.06 wt%) remain in the CR-CoOOH bulk sample, while XPS and EDS (Fig. S3, S9) show no detectable V on the surface. This suggests the trace residues are confined within the bulk. The DFT model of CR-CoOOH (Fig. S38) assumes a pure, dopant-free CoOOH lattice with vacancies. Given that coordinatively unsaturated Co sites are energetically metastable, the potential role of these trace atoms in stabilizing these active defect sites is not addressed in the main text or Supplementary Information.

2. Lack of MEA Post-Mortem Analysis at High Currents: While the study reports stability at high current densities (up to 6 A/cm2), operating at such conditions typically induces mass and heat transport issues that can chemically or mechanically degrade the anion exchange membrane and the catalyst-ionomer interface. Although the structural state of the catalyst itself is analyzed post-operation via XAS (Fig. S32), the structural integrity of the Membrane Electrode Assembly (MEA) cross-section is not investigated.

3. Generality of the Cascade-Reconstruction Strategy: The cascade reconstruction strategy and the SC-ROC mechanism are investigated specifically for the Co-based system. The manuscript lacks data or discussion on whether this design principle can be extended to other conventional OER catalyst systems, such as Ni- or Fe-based materials.

Comments and suggestions

1. Clarification on the Role of Trace Residues: To align the experimental composition with the theoretical model, the authors should clarify the potential stabilizing role of the trace V/S residues. This can be addressed by providing atomic-resolution STEM-EELS mapping to specify the location of the residues, or by adding a DFT discussion on whether a single V/S atom near a vacancy alters the local thermodynamic stability and spin-polarization.

2. Post-Mortem Analysis of the MEA: To verify the device-level durability under high-current AEMWE operations, the authors should provide a post-mortem cross-sectional SEM/EDS analysis of the MEA. Verifying the physical and chemical integrity of the membrane and the catalyst layer interface after the high-current stability test is required.

3. Perspective on Broader Applicability: To evaluate the general applicability of this approach, it would be beneficial to address its universality. We suggest the authors discuss or provide preliminary data on whether this cascade-reconstruction strategy can be extended to other conventional OER catalysts (e.g., V-doped NiS2).

The development of the CR-CoOOH catalyst via a cascade reconstruction strategy provides a functional approach to designing OER electrocatalysts. The operando characterizations and the analysis of the SC-ROC mechanism offer relevant mechanistic data. However, the authors need to address the remaining analytical gaps regarding the exact role of trace residues in the lattice and the comprehensive MEA structural stability under high-current conditions. We recommend the publication of this manuscript after a Major Revision addressing the comments raised above.

Response:

1. Clarification on the Role of Trace Residues: To align the experimental composition with the theoretical model, the authors should clarify the potential stabilizing role of the trace V/S residues. This can be addressed by providing atomic-resolution STEM-EELS mapping to specify the location of the residues, or by adding a DFT discussion on whether a single V/S atom near a vacancy alters the local thermodynamic stability and spin-polarization.

Response: We thank the reviewer for this thoughtful suggestion. We would like to first clarify the rationale for constructing the V/S-free CR-CoOOH model in our DFT calculations. As shown in the CoS_2 Pourbaix diagram (Fig. R3-1), under alkaline anodic conditions relevant to OER, the thermodynamically stable cobalt-containing solid phase is $CoHO_2(s)$, corresponding to a CoOOH-like oxyhydroxide phase. This indicates that the sulfide precursor is expected to reconstruct into a CoOOH-type active phase under OER conditions. Therefore, the reconstructed CoOOH phase was selected as the active-phase model in our DFT calculations.

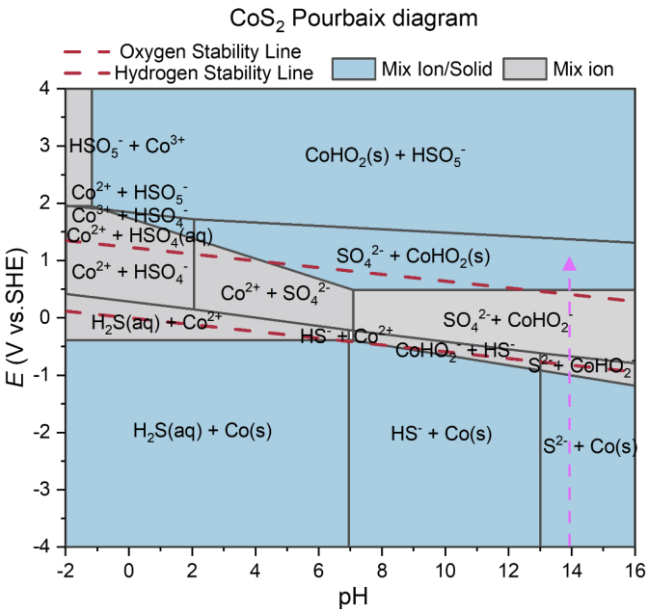

Fig. R3-1 | Pourbaix-diagram analysis of the thermodynamically stable phase under alkaline OER conditions. (Supplementary Fig. 45 in revised manuscript)

This thermodynamic assignment is also consistent with our experimental compositional analyses. The time-dependent XPS spectra show the progressive removal of V and S during electrochemical reconstruction, accompanied by the formation of the CoOOH phase (Fig. R3-2). In the revised work, we further conducted time-dependent ICP analysis with a longer electrochemical oxidation time. After prolonged electrochemical reconstruction for 10 h, both V and S signals become undetectable within the detection limits of our compositional analysis, confirming the nearly complete removal of these elements from the reconstructed catalyst (Table R3-1). These results indicate that V and S mainly serve as sacrificial components to trigger cascade reconstruction, rather than as final catalytic active components. Based on these results, the V/S-free reconstructed CoOOH model was used to represent the dominant active motif of the working catalyst.

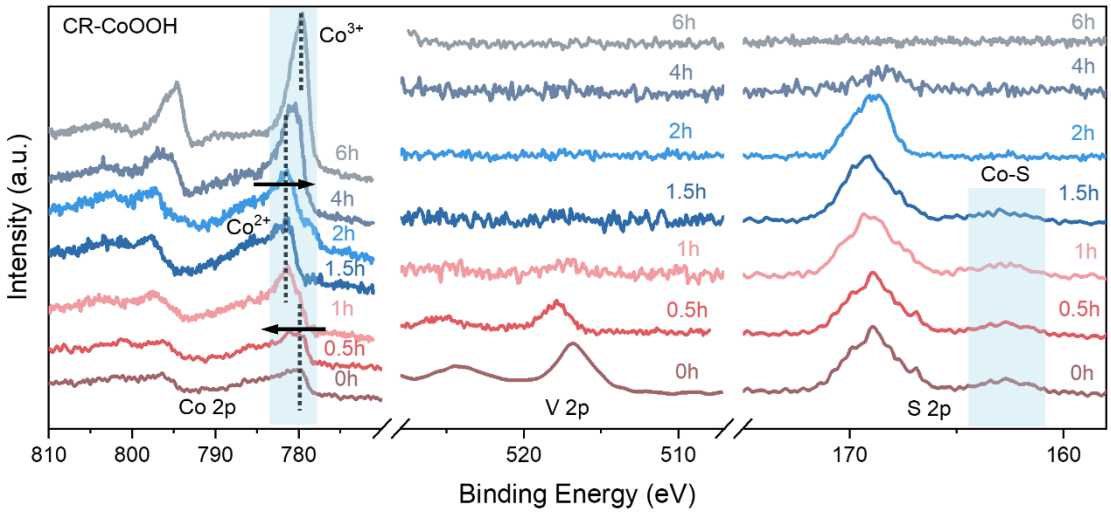

Fig. R3-2 | High-resolution Co 2*p*, V 2*p*, and S 2*p* XPS spectra of CR-CoOOH recorded after different electrochemical activation times (0-6 h). (Supplementary Fig. 4 in revised manuscript)

V-CoS_2 Stage	Mass ratio of Co (wt%)	Mass ratio of S (wt%)	Mass ratio of V (wt%)
0 h	37.92	27.63	3.02
2 h	20.28	0.28	0.25
4 h	20.03	0.23	0.19
6h	19.96	0.06	0.03
10 h	21.55	NA	NA

Table. R3-1| Time-dependent ICP analysis after prolonged electrochemical reconstruction.

We also considered atomic-resolution STEM-EELS mapping to directly locate trace V/S residues. However, reconstructed CoOOH-type oxyhydroxides are sensitive to electron-beam exposure under atomic-resolution STEM/TEM conditions. As shown in Fig. R3-3, after high-resolution electron-beam exposure, lattice fringes assignable to Co_3O_4 can be observed, indicating partial beam-induced transformation of the reconstructed oxyhydroxide phase. Therefore, atomic-resolution STEM-EELS mapping under such conditions may not reliably reflect the native CR-CoOOH structure or the real spatial distribution of trace V/S residues.

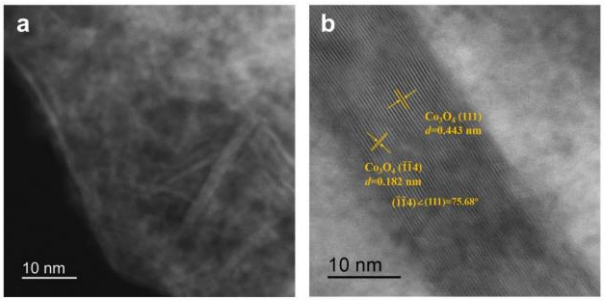

Fig. R3-3 | Atomically-resolved STEM images of S-CoOOH. a Atomicallyresolved STEM-HAADF (scanning transmission electron microscopy - high-angle annular dark field) image of S-CoOOH. b Atomically-resolved STEM-ABF (scanning transmission electron microscopy - annular bright field) image of S-CoOOH. (Supplementary Fig. 14 from ***Nature Communications, 2024, 15(1): 1383.***)

According to the reviewers suggestion, we performed STEM-EDS and STEM-EELS elemental mapping on CR-CoOOH. As shown in Fig. R3-4, the STEM-EDS elemental maps reveal that Co and O are evenly distributed throughout the reconstructed CR-CoOOH region. In contrast, negligible S and V signals are observed, suggesting that sulfur- and vanadium-containing species are completely removed during electrochemical reconstruction. Consistently, the STEM-EELS spectrum imaging results in Fig. R3-5 confirm the negligible V *L*-edge and S *L*-edge signals.

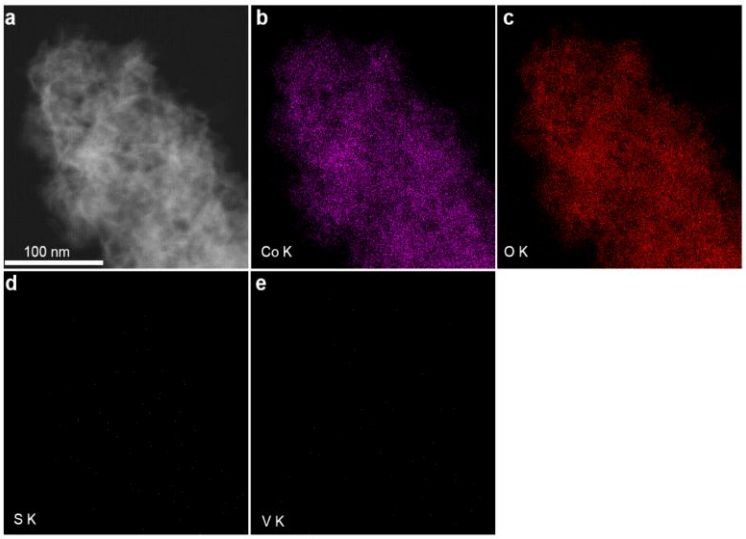

Fig. R3-4 | STEM–EDS elemental mapping of CR-CoOOH. (a) HAADF-STEM image of CR-CoOOH and the corresponding EDS elemental maps of (b) Co, (c) O, (d) S, and (e) V. (Supplementary Fig. 11 in revised manuscript)

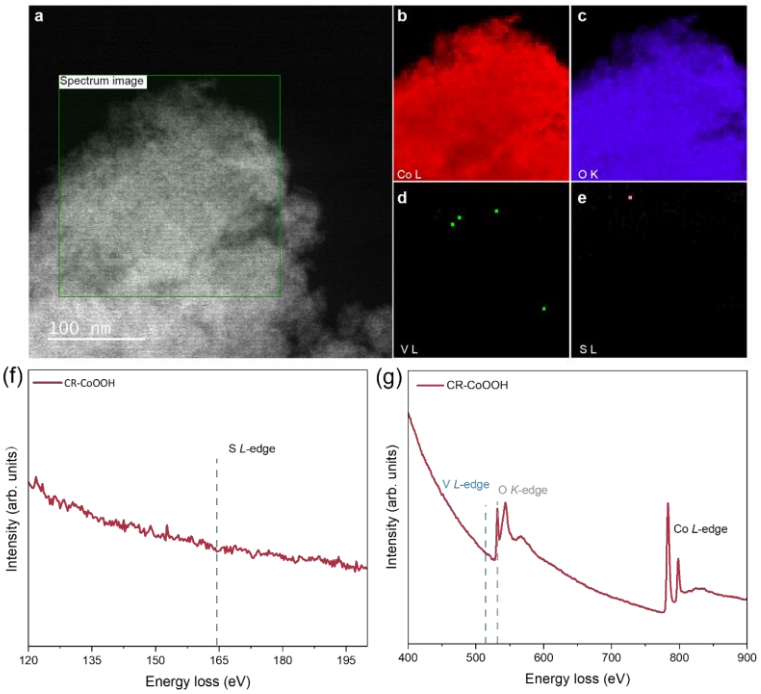

Fig. R3-5 | STEM–EELS characterization of CR-CoOOH. (a) HAADF-STEM image of CR-CoOOH with the selected spectrum-imaging region marked by the green box. Corresponding EELS elemental maps of (b) Co *L*-edge, (c) O *K*-edge, (d) V *L*-edge, and (e) S *L*-edge acquired from the selected region. (Supplementary Fig. 12 in revised manuscript)

To further clarify whether trace V/S-derived species could play an activity-enhancing role, we performed additional control experiments. After reconstruction, the CR-CoOOH electrode was thoroughly rinsed and transferred to fresh 1 M KOH for OER testing, and the polarization curve remained nearly unchanged (Fig. R3-6a). Moreover, deliberate addition of vanadate and sulfate ions into fresh 1 M KOH caused negligible

changes in the OER activity of CR-CoOOH (Fig. R3-6b). These results indicate that soluble or weakly adsorbed V/S-derived species do not measurably affect the catalytic performance.

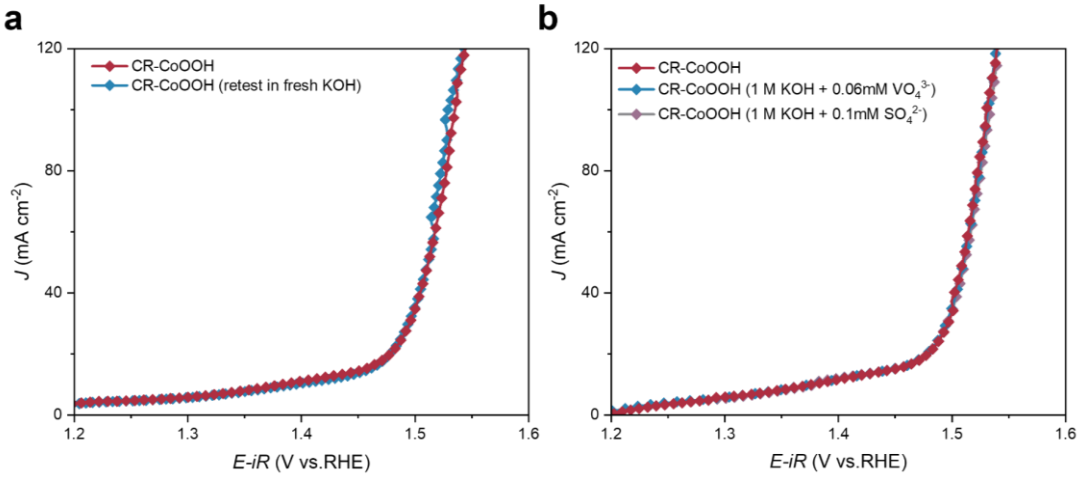

Fig. R3-6 | Control experiments excluding the activity contribution of soluble or weakly adsorbed V/S-derived species. a, OER polarization curves of CR-CoOOH measured before and after transferring the reconstructed electrode into fresh 1 M KOH. **b,** OER polarization curves of CR-CoOOH measured in fresh 1 M KOH with and without deliberately added vanadate and sulfate ions. (Supplementary Fig. 33 in revised manuscript)

Following the reviewer's suggestion, we further examined a simplified DFT model containing residual V/S species near coordination-unsaturated Co–O sites. For these trace-residue configurations, we focused on whether residual V/S species qualitatively alter the spin-density distribution relevant to the proposed SC-ROC mechanism. As shown in Fig. R3-7, the V/S-containing model does not show a qualitatively different spin-density distribution from the V/S-free CR-CoOOH model. The spin density remains mainly associated with the defective Co–O network, rather than being dominated by residual V/S atoms. This comparison indicates that residual V/S species do not generate the key spin-polarized Co–O electronic structure, supporting that the spin-polarizable Co–O states originate primarily from cascade-reconstruction-induced Co–O coordination reconfiguration.

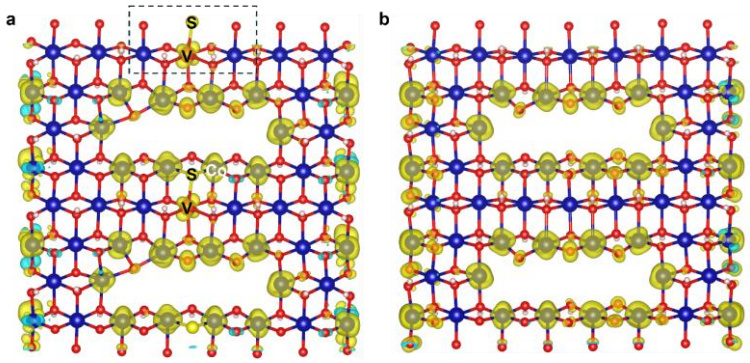

Fig. R3-7 | Spin-density comparison of V/S-containing (**a**) and V/S-free CR-CoOOH models (**b**). (Supplementary Fig. 47 in revised manuscript)

To further experimentally examine whether V incorporation itself can induce the spin-polarized electronic structure, we synthesized V-doped CoOOH as a control sample and performed EPR characterization (Fig. R3-8). In contrast to CR-CoOOH, V-doped CoOOH does not show the characteristic Co-centered unpaired-

spin signal at g = 2.16. This result indicates that V incorporation alone cannot account for the unpaired-spin feature observed in CR-CoOOH. Therefore, the observed spin-polarized Co–O electronic structure originates primarily from cascade-reconstruction-induced Co–O coordination reconfiguration, rather than from residual V/S species.

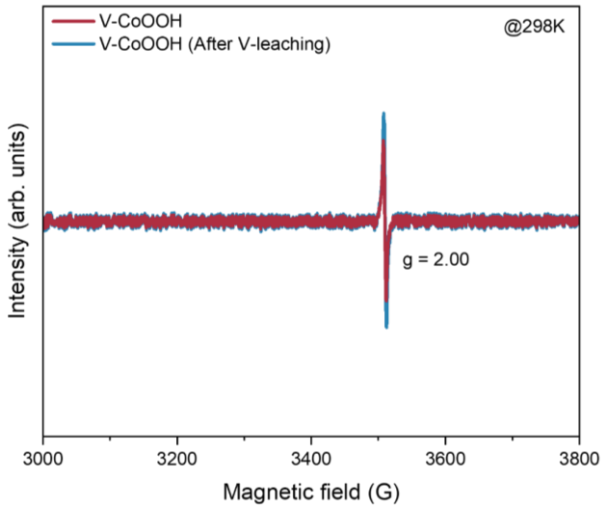

Fig. R3-8 | EPR characterization of V-CoOOH before and after electrochemical V-leaching. (Supplementary Fig. 22a in revised manuscript)

To address the comment, we have revised our manuscript as follows

(line 138, page 4, highlighted in yellow): The structural transformation of V-CoS_2 under anodic conditions was further validated by ex situ structural and compositional analyses, including XRD, XPS and electron microscopy (Supplementary Fig.6-12). These results consistently indicate extensive conversion of the V-CoS_2 precursor into a reconstructed CoOOH phase, accompanied by the near-complete removal of V and S species. To further quantify the compositional evolution, time-dependent ICP analysis was conducted after prolonged electrochemical reconstruction. After 10 h activation, both V and S become undetectable within the detection limits (Supplementary Table 1), further confirming that these elements are not retained as stable components in the reconstructed catalyst. This compositional evolution supports that V and S primarily participate in triggering the reconstruction process, rather than serving as final catalytic active components.

(line 234, page 7, highlighted in yellow): In particular, V–CoOOH does not show the characteristic $g \approx 2.16$ signal even after electrochemical V leaching, further excluding residual V incorporation as the origin of the spin-polarizable Co–O electronic structure.

(line 298, page 9, highlighted in yellow): To rule out possible contributions from soluble vanadate and sulfate species generated during reconstruction, the OER polarization curve was remeasured after transferring the reconstructed CR-CoOOH electrode into fresh 1 M KOH electrolyte (Supplementary Fig.33a). The nearly unchanged LSV response indicates that species accumulated in the electrolyte during reconstruction are not responsible for the observed activity. We then deliberately added 0.06 mM vanadate and 0.1 mM sulfate ions into fresh 1 M KOH and repeated the OER measurement (Supplementary Fig. 33b). The negligible change in the polarization curve further shows that soluble V/S-derived species at these concentrations do not measurably affect the OER activity of CR-CoOOH.

(line 445, page 13, highlighted in yellow): The CR-CoOOH model was constructed without V or S to represent the dominant reconstructed CoOOH active phase identified experimentally. This model choice is also supported by the CoS_2 Pourbaix-diagram analysis, which shows that under alkaline anodic OER

conditions the thermodynamically stable cobalt-containing solid phase is $CoHO_2$(s), corresponding to a CoOOH-like oxyhydroxide phase (Supplementary Fig.45).

(line 504, page 15, highlighted in yellow): To further evaluate whether residual V/S species or V incorporation could account for the spin-polarized electronic structure, we performed two additional control calculations. First, a simplified V/S-containing CR-CoOOH model was constructed by placing residual V/S species near coordination-unsaturated Co–O sites. Compared with the V/S-free CR-CoOOH model, this V/S-containing model does not show a qualitatively new V/S-dominated spin-density distribution; instead, the spin density remains mainly associated with the defective Co–O network (Supplementary Fig. 47).

2. Post-Mortem Analysis of the MEA: To verify the device-level durability under high-current AEMWE operations, the authors should provide a post-mortem cross-sectional SEM/EDS analysis of the MEA. Verifying the physical and chemical integrity of the membrane and the catalyst layer interface after the high-current stability test is required.

Response: We thank the reviewer for this valuable suggestion. To verify the device-level durability of CR-CoOOH under high-current AEMWE operation, we performed post-mortem cross-sectional SEM/EDS analysis of the MEA after the stability test.

As shown in Fig. R3-9, the cross-sectional SEM image of the used MEA shows that the membrane and catalyst layers remain physically integrated after operation at 1 A cm^{-2} for 100 h, without obvious interfacial delamination or catastrophic collapse. The anode catalyst layer maintains intimate contact with the anion-exchange membrane, indicating good interfacial mechanical stability during prolonged water electrolysis. The corresponding cross-sectional EDS mapping further confirms the chemical integrity of the MEA. The Co signal is mainly confined to the anode catalyst layer, while the Pt signal is primarily distributed on the cathode side. No obvious Co migration across the membrane or severe catalyst-layer detachment is observed after the stability test. These results indicate that the CR-CoOOH anode layer remains chemically and spatially stable during AEMWE operation.

We also performed post-mortem top-view SEM/EDS analysis of the anode catalyst layer. The used CR-CoOOH electrode retains a continuous catalyst-layer morphology, and the Co and O signals remain broadly distributed over the electrode surface. This further confirms that the reconstructed oxyhydroxide catalyst layer is largely preserved after high-current operation.

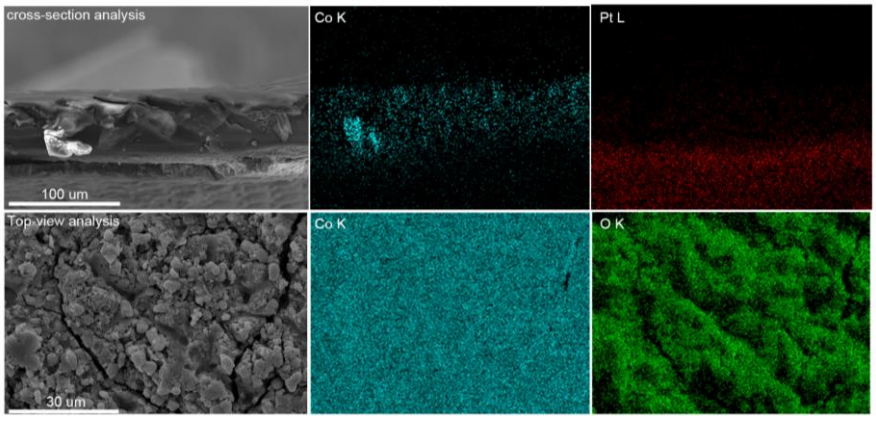

Fig. R3-9 | SEM/EDS analysis of the MEA after AEMWE stability testing. Cross-sectional SEM image and corresponding Co *K* and Pt *L* elemental maps of the used MEA after operation at 1 A cm^{-2} for 100 h.

Top-view SEM image and corresponding Co *K* and O *K* elemental maps of the used anode catalyst layer. The catalyst layer/membrane interface remains physically integrated, and the elemental distributions show no obvious Co migration across the membrane or severe catalyst-layer detachment after operation. (Supplementary Fig. 37 in revised manuscript)

Together with the stable cell-voltage profile during the AEMWE durability test, the post-mortem SEM/EDS results verify the physical and chemical robustness of the MEA and support the device-level durability of CR-CoOOH under high-current alkaline membrane water electrolysis.

To address the comment, we have revised our manuscript as follows (line 336, page 10, highlighted in yellow): Cross-sectional and top-view SEM/EDS analyses of the used MEA after stability testing further show that the catalyst layer/membrane interface remains physically integrated and that Co is mainly confined to the anode catalyst layer, with no obvious migration across the membrane (Supplementary Fig. 37).

3. Perspective on Broader Applicability: To evaluate the general applicability of this approach, it would be beneficial to address its universality. We suggest the authors discuss or provide preliminary data on whether this cascade-reconstruction strategy can be extended to other conventional OER catalysts (e.g., V-doped NiS_2).

Response: We thank the reviewer for this constructive suggestion. From an electronic-structure perspective, the proposed strategy may be extendable to other transition-metal oxyhydroxides (MOOH) beyond CoOOH if the MOOH can simultaneously provide oxygen-hole formation, spin-active metal 3*d* states, and adjacent oxygen-coupling geometry. For Ni-based oxyhydroxides, coordinatively unsaturated Ni–O units may also provide electronically favorable motifs for O–O coupling. From a ligand-field perspective, reducing the Ni–O coordination can lower the local symmetry of NiO_{6-x} units and perturb the splitting and occupancy of Ni e_g-derived states, which are directly involved in σ-type Ni e_g–O 2*p* hybridization. Such perturbation may facilitate the participation of O 2*p*-derived ligand-hole states in oxygen redox. More importantly, when these oxygen-derived hole states are coupled with partially occupied Ni e_g-derived states through Ni–O covalency, *p*–*d* exchange interactions may provide a possible route for spin polarization of oxygen-centered radicals. Therefore, coordinatively unsaturated Ni–O units are, in principle, plausible motifs for activating radical O–O coupling.

To provide preliminary proof-of-concept evidence for this possibility, we further constructed a Ni-based analogue by reconstructing V-NiS_2 into CR-NiOOH. As shown in Fig. R3-10, CR-NiOOH exhibits enhanced OER activity compared with LR-NiOOH and pristine NiOOH. Moreover, isotope-labeling DEMS shows a pronounced m/z = 36 signal for ^{18}O-labeled CR-NiOOH, whereas ^{18}O-labeled NiOOH shows negligible m/z = 36 response (Fig. R3-11). These results indicate that cascade reconstruction can also activate oxygen participation and O–O coupling in a NiOOH-based system.

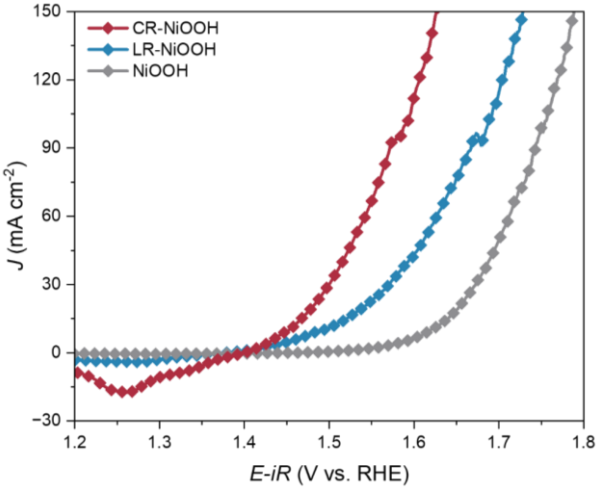

Fig. R3-10 | LSV curves of CR-NiOOH, LR-NiOOH, and NiOOH in fresh 1 M KOH. (Supplementary Fig. 50 in revised manuscript)

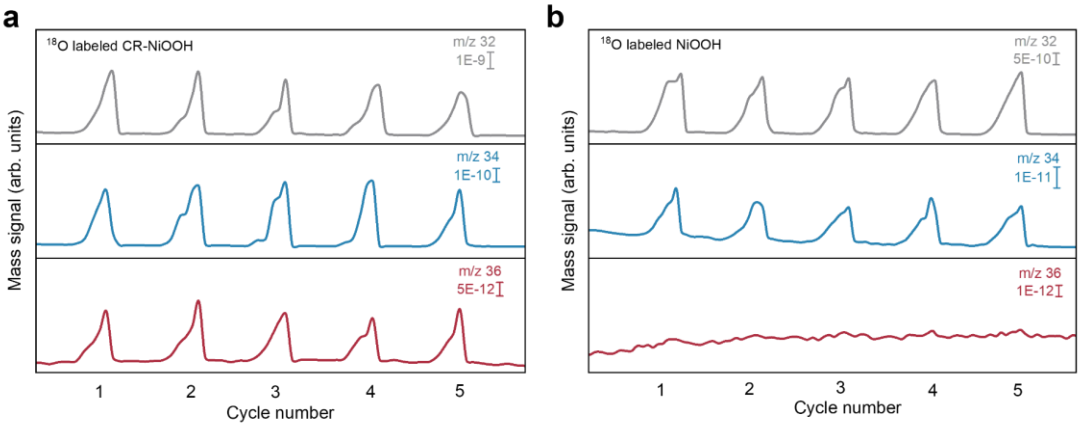

Fig. R3-11 | Operando DEMS characterization. a Operando DEMS signals of O_2 products for ^{18}O-labeled CR-NiOOH. **b** Operando DEMS signals of O_2 products for ^{18}O-labeled NiOOH. (Supplementary Fig. 51 in revised manuscript)

We note that this Ni-based experiment serves as preliminary proof-of-concept evidence for the broader applicability of the reconstruction-enabled oxygen-redox strategy. Full validation of spin-conserved coupling in non-Co systems would require further spin-sensitive characterizations and theoretical analysis. Accordingly, we have revised the manuscript to avoid overclaiming universality and added the Ni-based control data as supporting evidence for the potential extension of this cascade-reconstruction strategy beyond CoOOH.

To address the comment, we have revised our manuscript as follows (line 555, page 16, highlighted in yellow): Although this work focuses on a Co-based reconstructed oxyhydroxide, the underlying design concept may be extendable to other transition-metal oxyhydroxides if the reconstructed MOOH phase can provide oxygen-hole formation, spin-active metal 3*d* states, and adjacent oxygen-coupling geometry. For Ni-based oxyhydroxides, coordinatively unsaturated Ni–O units may perturb the local ligand field and modulate Ni e_g–O 2*p* hybridization, thereby facilitating oxygen-redox participation and radical O–O coupling. As preliminary proof-of-concept evidence, we constructed a Ni-based analogue by reconstructing

V-NiS_2 into CR-NiOOH. CR-NiOOH exhibits enhanced OER activity compared with LR-NiOOH and pristine NiOOH (Supplementary Fig. 50). Isotope-labeling DEMS shows a pronounced m/z = 36 signal for ^{18}O-labeled CR-NiOOH, whereas ^{18}O-labeled NiOOH shows negligible response, indicating reconstruction-enabled oxygen participation and O–O coupling in a NiOOH-based system (Supplementary Fig. 51). For Fe-based oxyhydroxides, spin-active Fe 3*d* states may also provide a possible exchange channel for polarizing oxygen-derived intermediates if suitable Fe–O coordination and oxygen-hole states can be engineered. Nevertheless, full validation of SC-ROC in non-Co systems requires further spin-sensitive characterization and theoretical analysis.

Reviewer #4 (Remarks to the Author):

The manuscript titled "Spin-conserved oxygen-redox coupling enables durable anion exchange membrane water electrolysis" by H. Li et al. reports the synthesis of reconstructed CoOOH with a high density of coordinatively unsaturated Co sites (denoted as CR-CoOOH) and evaluates its electrochemical oxygen evolution reaction (OER) performance. In addition, the authors performed several operando spectroscopic and XMCD measurements to investigate the OER mechanism. Finally, spin-polarized density functional theory (DFT) calculations were carried out to understand the microscopic electronic structure associated with the spin-conserved radical oxygen coupling (SC-ROC) mechanism in CR-CoOOH.

Overall, the authors provide substantial experimental evidence demonstrating that CR-CoOOH exhibits superior OER performance compared to pristine CoOOH and localized reconstructed CoOOH (LR-CoOOH). It is particularly impressive that, beyond the electrochemical measurements, the authors performed state-of-the-art operando spectroscopic studies, which are highly valuable for understanding the OER mechanism. Additionally, the manuscript is generally well written and clearly presented.

However, I find that the XMCD results and their interpretation are not fully convincing. Although the room-temperature magnetic measurements shown in Fig. 2g suggest weak ferromagnetism in CR-CoOOH, the Co L-edge XMCD spectra do not show the typical characteristics of ferromagnetic behavior. In conventional XMCD measurements of ferromagnetic materials, the dichroic signals at the L3 and L2 edges are expected to exhibit opposite signs. However, in Fig. 4f, the XMCD signals at both the L3 and L2 edges appear to have the same sign (positive). The authors should address this point more carefully. Is this behavior related to experimental artifacts (e.g., background subtraction or normalization procedures), or does it originate from intrinsic electronic or magnetic properties of the material? If the latter is the case, the authors should explain why the observed XMCD line shape differs from the commonly reported ferromagnetic XMCD features.
Response: We thank the reviewer for pointing out this important issue. We have carefully re-examined the Co *L*-edge XMCD data and the corresponding data-processing procedure. In the previous version, the weak dichroic difference was not sufficiently distinguished from the field-dependent background, which led to an ambiguous line shape. To avoid overinterpretation, we have reprocessed the spectra using consistent pre-edge background subtraction and post-edge normalization procedures for the absorption spectra collected under opposite magnetic fields.

In the Fig. R4-1, the reference CoOOH sample shows only a very weak difference signal after magnetic-field reversal. However, this signal is close to the noise level and does not show the characteristic opposite-sign features between the Co L_3 and L_2 edges. Therefore, it cannot be unambiguously assigned to an intrinsic XMCD response and may originate from field-dependent systematic background during magnetic-field reversal. Accordingly, the present Co *L*-edge XMCD measurement does not provide clear evidence of resolvable Co 3*d* spin polarization or magnetization in CoOOH. In contrast, CR-CoOOH exhibits a much clearer XMCD response. The extracted XMCD spectrum is smoother and shows clear opposite-sign features at the Co L_3 and L_2 edges, consistent with the characteristic line shape of transition-metal *L*-edge XMCD. This field-dependent dichroism can also be identified from the raw and background-subtracted spectra, where the field-induced intensity changes at the Co L_3 and L_2 edges show opposite trends. These opposite field-dependent variations at the L_3 and L_2 edges support the presence of an intrinsic XMCD signal in CR-CoOOH.

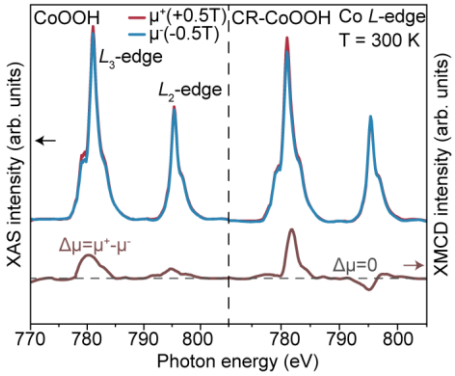

Fig. R4-1 | Co *L*-edge XAS and XMCD measurements of CoOOH and CR-CoOOH at 300 K. (Fig. 4f in revised manuscript)

Therefore, the revised XMCD results indicate that the detectable Co *L*-edge dichroic response is associated with CR-CoOOH rather than the reference CoOOH. The corrected Co *L*-edge XMCD result, together with the EPR, magnetic measurements, O *K*-edge XMCD, and DFT spin-density analysis, supports the formation of spin-polarizable Co–O electronic states in CR-CoOOH.

To address the comment, we have revised our manuscript as follows
(line 422, page 12, highlighted in yellow): For pristine CoOOH, the μ^+ and μ^- XAS spectra nearly overlap at the Co *L*-edge, and the extracted difference signal is close to the noise level without a clear opposite-sign feature between the Co L_3 and L_2 edges. Therefore, the Co *L*-edge XMCD data do not provide clear evidence of resolvable Co 3*d* spin polarization in pristine CoOOH. In contrast, CR-CoOOH exhibits a clear Co *L*-edge XMCD response after consistent pre-edge background subtraction and post-edge normalization. The dichroic signal shows opposite signs at the Co L_3 and L_2 edges, supporting the presence of spin-polarized Co 3*d* states in CR-CoOOH.

In addition, regarding the XMCD measurements, did the authors apply an external magnetic field to polarize the sample during the measurements? If so, what was the magnitude and direction of the applied magnetic field relative to the sample geometry?
Response: Thank you for your valuable comment. An external magnetic field was applied during all XMCD measurements to magnetically polarize the samples. The measurements were performed in the total electron yield (TEY) mode under normal incidence (90° with respect to the sample surface). The incident circularly polarized X-ray beam was parallel to the applied magnetic field, and the magnetic field was alternated between +0.5 T and −0.5 T during the measurements to obtain the XMCD spectra. The degree of circular polarization of the incident X-rays was greater than 99%, ensuring a high sensitivity to the magnetic polarization of the samples. All XMCD spectra were collected under the same experimental geometry and were processed using an identical normalization procedure to enable reliable comparison between different samples.

To address the comment, we have revised our manuscript as follows (line 625, page 18, highlighted in yellow): XMCD measurements were acquired at the Shanghai Synchrotron Radiation Facility in total electron yield (TEY) mode under normal incidence geometry, with the incident circularly polarized X-ray beam parallel to the applied magnetic field. An external magnetic field of ±0.5 T was applied and alternated during the measurements to obtain the XMCD spectra. The degree of circular polarization of the incident X-

rays was greater than 99%. All XMCD spectra were collected under the same experimental geometry and processed using identical normalization procedures for comparison.

From the perspective of practical device applications, it would also be valuable if the authors could provide further discussion regarding the scalability and stability of CR-CoOOH. Although the material shows superior electrochemical performance, are there any potential concerns regarding the industrial implementation of magnetic CoOOH-based materials, such as safety, stability, or large-scale manufacturability? Furthermore, how stable is the CR-CoOOH phase after synthesis and during long-term storage or operation?

Response: We thank the reviewer for this valuable suggestion. We have added a discussion on the scalability, safety, and stability of CR-CoOOH from the perspective of practical AEMWE applications.

First, regarding scalability and manufacturability, the preparation of CR-CoOOH is based on conventional sulfide synthesis followed by electrochemical reconstruction in alkaline electrolyte. This process does not require noble metals, high-vacuum treatment, or complex nanofabrication steps, suggesting potential compatibility with scalable electrode fabrication. In addition, the reconstruction is conducted under anodic operating conditions similar to OER activation, which means that the active CR-CoOOH phase can be generated directly on the anode electrode within the MEA during electrochemical activation. Therefore, the synthetic route is, in principle, compatible with practical electrode preparation, although further optimization of large-area loading uniformity, activation time, and electrode architecture will be required for industrial-scale implementation.

Second, CR-CoOOH is not a strongly magnetic bulk ferromagnet. The observed weak magnetic response reflects local spin-polarizable Co–O electronic states and is not expected to introduce additional magnetic-safety concerns during AEMWE operation. For practical scale-up, an important consideration would be to maximize the density and accessibility of these active Co–O motifs in large-area electrodes.

Third, regarding phase stability, CR-CoOOH shows good operational stability under both three-electrode OER testing and device-level AEMWE operation. To further verify the MEA integrity after high-current operation, we have added cross-sectional and top-view SEM/EDS analyses of the used MEA after the stability test (Fig. R4-2). The catalyst layer and membrane remain physically integrated, without obvious interfacial delamination or catastrophic collapse, and the EDS maps show that Co is mainly confined to the anode catalyst layer with no obvious migration across the membrane. The top-view SEM/EDS results further confirm that the used anode catalyst layer maintains a continuous morphology with broadly distributed Co and O signals. These results indicate that the reconstructed CoOOH catalyst layer and the catalyst/membrane interface are largely preserved during AEMWE operation.

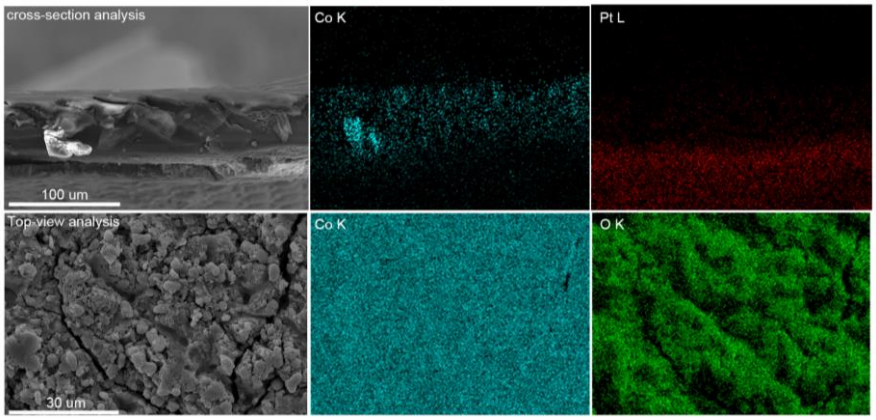

Fig. R4-2 | SEM/EDS analysis of the MEA after AEMWE stability testing. Cross-sectional SEM image and corresponding Co *K* and Pt *L* elemental maps of the used MEA after operation at 1 A cm^{-2} for 100 h. Top-view SEM image and corresponding Co *K* and O *K* elemental maps of the used anode catalyst layer. The catalyst layer/membrane interface remains physically integrated, and the elemental distributions show no obvious Co migration across the membrane or severe catalyst-layer detachment after operation. (Supplementary Fig. 37 in revised manuscript)

To address the comment, we have revised our manuscript as follows

(line 336, page 10, highlighted in yellow): Cross-sectional and top-view SEM/EDS analyses of the used MEA after stability testing further show that the catalyst layer/membrane interface remains physically integrated and that Co is mainly confined to the anode catalyst layer, with no obvious migration across the membrane (Supplementary Fig. 37).

(line 570, page 16, highlighted in yellow): From a practical application perspective, CR-CoOOH also offers potential compatibility with scalable AEMWE electrode fabrication. Its preparation relies on conventional sulfide synthesis followed by electrochemical reconstruction in alkaline electrolyte, without requiring noble metals, high-vacuum treatment, or complex nanofabrication. The reconstructed CR-CoOOH phase can be generated directly on the anode electrode during electrochemical activation, which is compatible with electrode-level preparation. Moreover, CR-CoOOH is not a strongly magnetic bulk ferromagnet; the observed weak magnetic response reflects local spin-polarizable Co–O electronic states and is not expected to introduce additional magnetic-safety concerns during AEMWE operation. For future scale-up, an important consideration will be to maximize the density and accessibility of these active Co–O motifs in large-area electrodes.

Response to referees

We thank the three referees for taking the time to carefully review the manuscript and for giving many useful suggestions. The manuscript has been revised according to their comments and the changes have been highlighted in the revised version. We feel the quality of the paper has been improved greatly thanks to the input from the referees. Below is a point-by-point response.

Reviewer #1 (Remarks to the Author):

The author has made revisions, and I believe the current version is acceptable.

Reviewer #2 (Remarks to the Author):

I appreciate the authors' responses to my comments and suggestions. I recommend acceptance of this manuscript for publication. I also suggest uploading the calculation-related coordinate files to the Supporting Information for reproducibility purposes.

Response: We thank the reviewer for this suggestion. We will upload the calculation-related coordinate information as a separate file.

Reviewer #3 (Remarks to the Author):

The manuscript has been substantially improved, and the authors have made considerable efforts to address the previous concerns. The responses regarding the role of residual V/S species and the broader applicability of the cascade-reconstruction strategy are satisfactory. However, the concern regarding the structural stability of the membrane electrode assembly under high-current-density operation has not yet been fully addressed.

1. Role of trace V/S residues

The authors have addressed the concern regarding the possible contribution of residual V and S species. The extended ICP-OES analysis, STEM-EDS/EELS characterization, electrochemical control experiments, V/S-containing DFT model, and EPR characterization of V-doped CoOOH collectively support the conclusion that residual V/S species are not the primary origin of the spin-polarized Co–O electronic structure.

These results also provide a reasonable justification for using a V/S-free reconstructed CoOOH model to represent the dominant active motif of the working catalyst.

2. Post-mortem analysis of the MEA under high-current-density operation

The authors have added cross-sectional and top-view SEM/EDS analyses of an MEA operated at 1 A cm-2 for 100 h. These results show that the catalyst layer and membrane remain physically integrated under this operating condition, without obvious Co migration across the membrane or severe catalyst-layer detachment. However, this experiment does not directly address the original concern regarding MEA stability under high-current-density operation. The manuscript highlights stable operation at 2, 4, and 6 A cm-2 for 100 h at each current density, whereas the post-mortem analysis was performed only after operation at 1 A cm-2 for 100 h. At current densities as high as 6 A cm-2, substantially greater gas evolution, local heating and mechanical stress may be generated within the MEA. These conditions may lead to catalyst-layer cracking, interfacial delamination, membrane deformation, catalyst migration, or local degradation that may not occur at 1 A cm^{-2}.

Therefore, additional post-mortem analysis of an MEA subjected to the reported high-current-density durability test is required. The authors should preferably analyze the MEA used for the sequential durability test at 2, 4, and 6 A cm-2, or alternatively perform a representative durability experiment at 6 A cm-2 followed by post-mortem characterization.

The currently provided 1 A cm-2, 100 h result is useful but cannot substitute for direct post-mortem evaluation under the high-current-density conditions emphasized in the manuscript. This comment therefore remains unresolved and requires additional experimental evidence.

3. Broader applicability of the cascade-reconstruction strategy

The authors have satisfactorily addressed the concern regarding the extension of the cascade-reconstruction strategy beyond the CoOOH system. The newly added CR-NiOOH results demonstrate enhanced OER activity relative to LR-NiOOH and pristine NiOOH. In addition, the isotope-labeling DEMS results provide reasonable preliminary evidence that cascade reconstruction can promote oxygen participation and O–O coupling in a Ni-based oxyhydroxide system. The authors have also appropriately acknowledged that these results do not fully demonstrate spin-conserved radical oxygen coupling in the Ni system and that further spin-sensitive characterization and theoretical analysis would be required. The revised discussion therefore avoids overclaiming the universality of the proposed mechanism.

Overall assessment

The revised manuscript has been significantly strengthened, and two of the three major concerns raised in the previous review have been satisfactorily resolved. Nevertheless, the structural integrity of the MEA under the reported high-current-density operating conditions remains insufficiently verified. Because high-current-density durability is one of the principal practical claims of this work, direct post-mortem characterization of an MEA operated at the reported high current densities is necessary.

Response: We thank the reviewer for this important comment. In the revised manuscript, we performed an additional high-current-density AEMWE durability test at 6 A cm^{-2} for 100 h, followed by cross-sectional SEM/EDS analysis of the used MEA.

As shown in Fig. R4-1, after operation at 6 A cm^{-2} for 100 h, the MEA retains an integrated cross-sectional structure. The catalyst layer remains in contact with the membrane, without obvious interfacial delamination, catastrophic collapse, or severe membrane deformation. The corresponding EDS elemental maps show that the Co and O signals are mainly confined to the anode catalyst layer, while the Pt signal remains localized on the cathode side. No obvious Co migration across the membrane or Pt crossover toward the anode side is observed.

These results directly verify the physical and chemical integrity of the MEA under the highest current-density condition used in this work. Together with the stable voltage profiles during high-current-density AEMWE operation, the cross-sectional SEM/EDS analysis confirms that the CR-CoOOH-based MEA maintains robust catalyst-layer/membrane interfaces without severe catalyst migration or structural degradation.

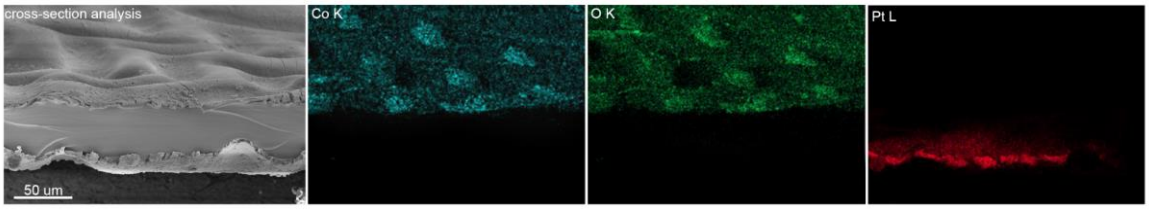

Fig. R4-1 | Cross-sectional SEM/EDS analysis of the MEA after operation at 6 A cm^{-2} for 100 h.

(Supplementary Fig. 38 in revised manuscript)

To address the comment, we have revised our manuscript as follows:

(line 336, page 10, highlighted in yellow): SEM/EDS analyses of the used MEAs after operation at 1 A cm^{-}

^{2} for 100 h and 6 A cm^{-2} for 100 h show that the catalyst layer/membrane interfaces remain physically integrated under both conditions (Supplementary Fig. 37-38). Notably, the MEA operated at 6 A cm^{-2} for 100 h shows no obvious interfacial delamination, severe membrane deformation, or catalyst migration across the membrane, directly confirming the structural integrity of the MEA under high-current-density operation (Supplementary Fig. 38).

Reviewer #4 (Remarks to the Author):

The authors have adequately addressed all of the reviewers' comments and revised the manuscript accordingly. I find the current version of the manuscript satisfactory and recommend that it be accepted for publication in its present form.